Steady State Analysis of Compensated Self Excited Induction Generator Using Fuzzy Logic

Thesis submitted in the partial fulfillment of the requirements for the award of the degree of

Masters of Engineering
in
Power Systems & Electric Drives

Thapar University, Patiala

By
Praveen Kumar Nirujogi
Roll No: 800841012

Under the supervision of

Dr. Sanjay K. Jain
Assistant Professor, EIED

Mr. S.S.S.R. Sarathbabu Duvvuri
Lecturer, EIED

JULY 2010

ELECTRICAL & INSTRUMENTATION ENGINEERING DEPARTMENT
THAPAR UNIVERSITY
PATIALA-147004

CERTIFICATE

I hereby certify that work which is being presented in the Thesis entitled **"Steady State Analysis of Compensated Self Excited Induction Generator Using Fuzzy Logic"** in partial fulfilment of the requirement for the award of degree of Master of Engineering in ***Power Systems & Electric Drives*** submitted in Electrical & Instrumentation Engineering Department of Thapar University, Patiala, is an authentic record of my own work carried out under supervision of **Dr. Sanjay K. Jain**, Asst. Prof., EIED and **Mr. S.S.S.R. Sarathbabu Duvvuri**, Lecturer, EIED.

The matter presented in this Thesis has not been submitted for the award of any other degree of this or any other university.

Praveen Kumar Nirujogi
(800841012)

It is certified that the above statement made by the student is correct to the best of our knowledge and belief.

Dr. Sanjay K. Jain
Assistant Professor, EIED
Thapar University, Patiala

Mr. S.S.S.R. Sarathbabu Duvvuri
Lecturer, EIED
Thapar University, Patiala

Countersigned by

Dr. Smarajit Ghosh
Professor & Head, EIED
Thapar University
Patiala

Dr. R. K. Sharma
Dean of Academic Affairs
Thapar University
Patiala

ACKNOWLEDGEMENT

First of all, I thank the Almighty, who gave me the opportunity and strength to carry out this work.

I would like to thank **Dr. Sanjay K. Jain, Assistant Prof., EIED** for the opportunity to work with him, and also for his encouragement, trust and untiring support. **Dr. Sanjay K. Jain** has been an advisor in the true sense both academically and morally throughout this project work.

I take this opportunity to express my gratitude and sincere thanks to **Mr. S.S.S.R. Sarathbabu Duvvuri, Lecturer, EIED** for his valuable advices and suggestions during the thesis work.

Gratitude is accorded to Thapar University, Patiala, for providing all the necessary facilities to complete my M.E. Thesis work.

I am thankful to **Dr. Smarajit Ghosh, Professor & Head, EIED** for his continuous inspiration during this thesis work.

The paucity of words does not compromise for extending my thanks to all the faculty and staff members of EIED, Thapar University and my all family members and friends whose uninterrupted love, inspiration and blessings helped me in completing this research report.

I thank and owe my deepest regards to all who have helped me directly or indirectly.

Praveen Kumar Nirujogi

Regn. No. 800841012

ABSTRACT

For the self excited induction generators (SEIG), both the frequency (F) and the magnetizing reactance (X_m) which depends upon magnetic saturation, vary with load even when the rotor speed is maintained constant. The performance of SEIG can be calculated if the $X_m$and F are determined accurately. Therefore, a crucial step in the steady-state analysis of the SEIG for the given machine parameter, speed**,** excitation capacitance and load impedance is to determine the value of the frequency (F) and the magnetizing reactance (X_m).

In the present work, a mathematical model employing the loop impedance method based on graph theory is used which results in simple formulation and is convenient for computer solution. The unknown magnetizing reactance (X_m) and frequency (F) has been computed using Fuzzy logic based algorithm. The frequency (F) and magnetising (X_m) are computed separately using real and imaginary parts. The effectiveness of the method is tested through the simulation for simple shunt SEIG and series capacitor compensated SEIGs i.e. short shunt and long shunt SEIGs. The effects of change in capacitance and prime mover speed are also simulated. The analysis presented is validated by experimental results.

TABLE OF CONTENTS

LIST OF FIGURES

CHAPTER – 1

INTRODUCTION

1.1 OVERVIEW

The generation of electrical energy mainly so far has been from thermal, nuclear, and hydro plants. They have continuously degraded the environmental conditions. An increasing rate of the depletion of conventional energy sources and the degradation of environmental conditions has given rise to an increased emphasis on renewable energy sources, particularly after the increases in fuel prices during the 1970s [1]. The renewable sources are advantageous due to their abundance availability and pollution less energy conversion.

For small capacity applications use of an induction machine as a generator is becoming more popular for the renewable sources. An **induction generator** is an externally driven induction machine. The Induction generator offers relatively certain advantages over a conventional synchronous generators such as simple and robust construction, inexpensive as compared to the conventional synchronous generator, minimal maintenance, inherent overload protection, requiring no brushes or commutators, less material costs because of the use of electromagnets rather than permanent magnets, lower size and weight at high frequency (~400 Hz) and filter components. For its simplicity, robustness, and small size per generated kW, and variable speed operation the induction generator is favoured for small hydro and wind power plants [2, 3]. It can play a major role for the electrification of far flung areas where the extension of national grid is not economical like remote families, village community, small agricultural applications and lighting and heating loads. For feeding critical locations like library, hospitals, computer centres, telephone exchange, marketing complexes etc.

Although induction generators have several advantages, it consumes reactive power which results in poor power factor and poor voltage regulation. Therefore, use of self excited induction generator has wider acceptance and the SEIG is dependent on the methodology to be adopted to overcome the poor voltage. In SEIG the shunt

capacitors connected at their terminals provide the required reactive power for self excitation. The schematic diagram of SEIG is shown in Fig. 1.1. SEIG may be built with single phase or three phase output and may supply AC loads or AC rectified autonomous loads [5].

For the cost effective solution, the improved voltage regulation can be achieved by using series capacitors in conjunction with shunt capacitors. The self excited induction generator performance for given capacitance and load can be evaluated after computing the unknowns, X_m and F. The parameters are calculated by intelligent technique, i.e. Fuzzy logic.

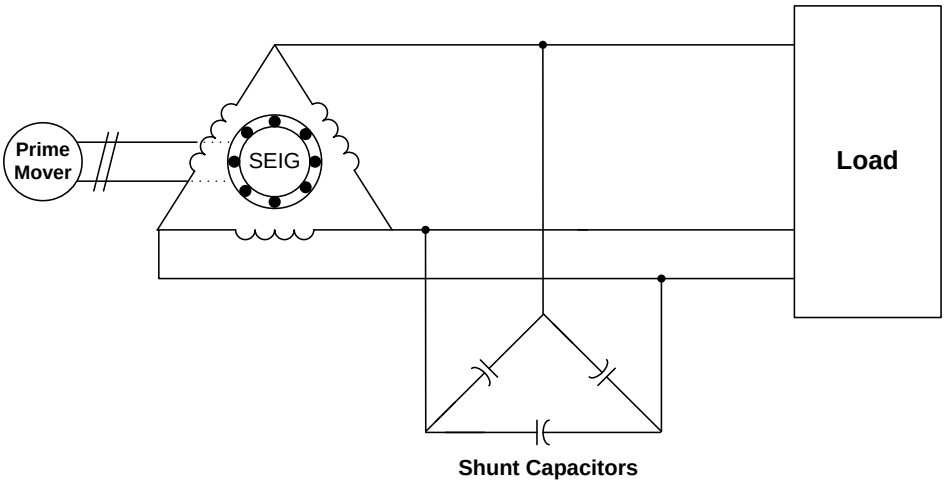

Fig. 1.1: Self-excited induction generator

In Fig. 1.1 a capacitor bank is connected across the stator terminals of a 3-phase induction machine which supply the reactive power to the induction generator for self excitement process and as well as to the load.

1.1.1 SELF EXCITATION IN SEIG

The self excited induction generator is the arrangement of externally driven induction machine having a capacity capacitor bank at stator terminals. The voltage building is achieved at no load and after the successful voltage building, the load is connected.

The process of voltage build up in self excited induction generator is similar to that in dc shunt generator this is explained with the help of Fig. 1.2. When the rotor of

induction machine is run at the required speed, residual magnetism present in the rotor iron generates a small terminal voltage ‘op’ across stator terminals. This voltage produces a capacitor current ‘oq’. The current ‘oq’ creates a flux which aid the residual flux, thus producing more flux and therefore results into higher voltage ‘qr’ across stator terminals. The voltage ‘qr’ results a current ‘os’ in the capacitor bank which eventually generates voltage ‘st’.

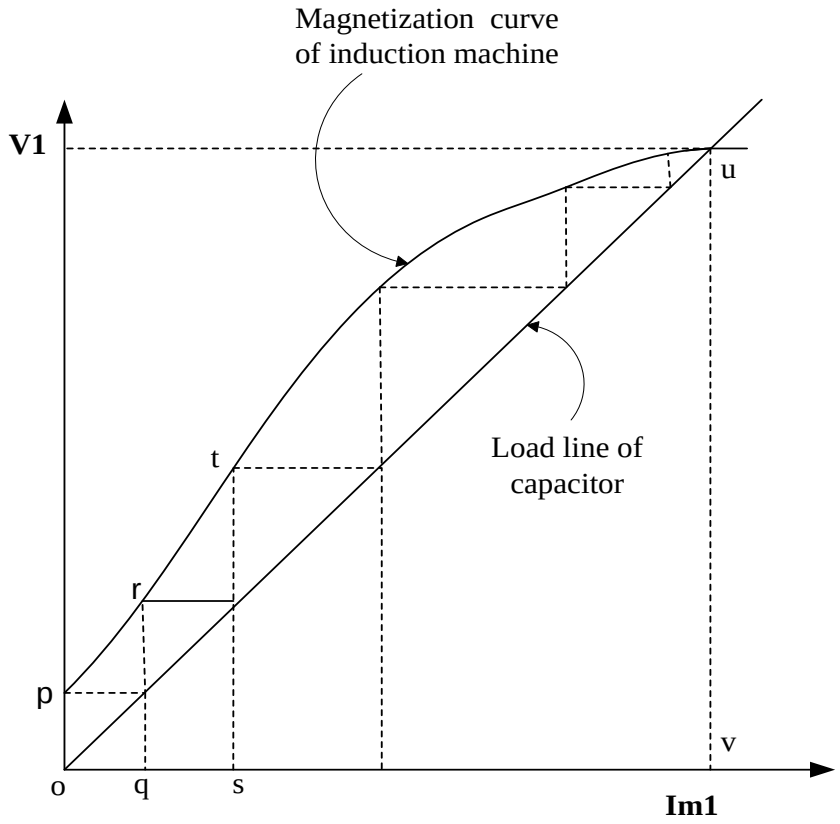

Fig. 1.2: Voltage building phenomenon in SEIG

The process of cumulative voltage build-up continues till the saturation curve of induction generator intersects the capacitor load line at point v, which results into no load voltage of ‘uv’ and magnetizing current I_m. The slope of load line due to capacitance is given by$\tan^{-1}(1/\omega C)$.

From Fig. 1.3 it has been observed that the voltage build up depends upon the value of capacitance, i.e. for the capacitance C1 the voltage produced is V1 and for the capacitance C2 (C2<C1) the voltage produced is V2 which is less than the voltage V1and for the C3 (C3<C2) the voltage build up is further reduced. Therefore, higher the capacitance, greater is the voltage build up and the lower the voltage for lower

capacitance. In case capacitor load line does not intersect the magnetization curve of induction machine, there would be no voltage build up. In Fig. 1.3, voltage build up for capacitor C4 does not occur.

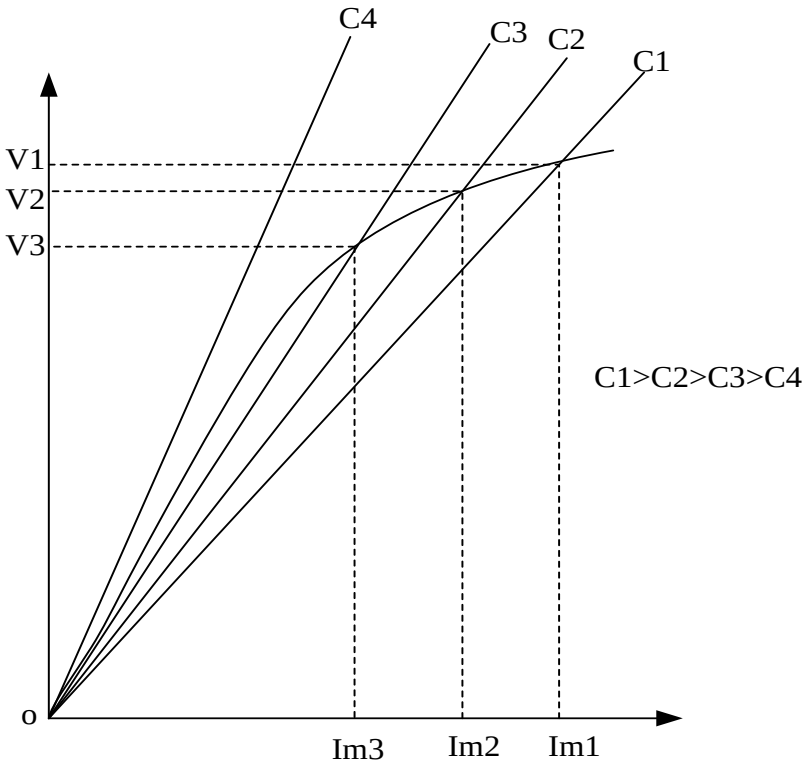

Fig. 1.3: Effect of capacitances on voltage build up process

Build up process depends upon its residual voltage which is nearly 6 volt to 10 volt for a 220 volt machine; a battery of small value can be connected across the rotor terminal to generate the residual voltage or residual flux into rotor iron, once a machine run as a generator residual magnetism remains for a few days. If the residual flux is absent in the rotor iron, the induction generator will not build up. This problem can be overcome by running the machine as a poly phase induction motor for some time to create residual magnetism.

1.2 LITERATURE SURVEY

Use of Induction generator has been increasing due to the exploitation of renewable energy resources and the development of autonomous power systems. Induction generator (IG) is cost effective, rugged, does not require external d.c supply and has inherent protection against short circuit. Reactive power consumption and

poor voltage regulation under varying frequency are the major drawbacks of the induction generators [10].

Mainly IGs are two types wound rotor IGs and squirrel cage IGs and further can be classified as grid connected and self exited IGs [4]. Depending upon their prime movers used and their locations these can be broadly classified as constant speed constant frequency (CSCF), variable speed constant frequency (VSCF) [6-9] and variable speed variable frequency (VSVF) [8]. For variable speed corresponding to the changing derived speed, SEIG can be conveniently used for resistive heating loads, which are essentially frequency insensitive. This section presents a review of the work reported in literature on the analysis of 3-phase self-excited induction generator (SEIG).

Self-excitation phenomenon in induction machines is a subject of considerable attention due to the application of SEIG in isolated power systems [12 -14]. Elder *et al.* [13] have presented the physical background of the self excitation process in induction generator. The process of voltage build-up in an SEIG is very much similar to that of a dc generator, there must be a suitable value of residual magnetism present in the rotor for the required voltage build-up. So for an isolated mode, there must be a suitable capacitor bank connected across the generator terminals. This phenomenon is known as capacitor self excitation and the induction generator are called as "SEIG". Ahmed *et al.* [15] have analysed SEIG behaviour for variable speed prime mover for minimum capacitance required for self excitation. Wang *et al.* [16] have presented an approach based on first-order eigen value sensitivity method to determine both maximum and minimum values of capacitance required for an isolated self-excited induction generator (SEIG) under different loading conditions.

In case of a grid-connected mode, the induction generator can draw reactive power either from the grid, but it will place a burden on the grid or by connecting a capacitor bank across the generator terminals [17].

The analysis of steady state performance of SEIG is of interest both from design and operational points of view. In an isolated power system, both the terminal voltage and frequency are unknown and have to be computed for a given speed,

capacitance, and load impedance. Over the past decade, many researchers have attempted to analyze the SEIG [18-].

Murthy *et al.* [18] have presented a mathematical model to obtain the steady-state performance of SEIG using the equivalent circuit impedance of the machine. The nonlinear equations corresponding to real and imaginary parts of the impedance, have been solved for two unknowns and using Newton–Raphson method. Quazene *et al.* [19] have used a nodal admittance technique to obtain a nodal equation and then separated it into its real and imaginary parts so as to solve them first for frequency (F) and then for magnetising reactance (X_m). Malik *et al*. [22] had considered the core loss component in the analysis and loop impedance model is used along with Newton-Raphson method to solve the unknown variables F and X_m. Rajakaruna *et al.* [27] have used an iterative technique which uses an approximate equivalent circuit and a mathematical model for B–H curve and the solution is reduced to a nonlinear equation in frequency (F). Singh *et al.* [28] tried an optimization technique by formulating this as a multivariate unconstrained nonlinear optimization problem. The impedance of the machine is taken as an objective function. The F and X_m are selected as independent variables, which are allowed to vary within their upper and lower limits so as to achieve practically acceptable values of the variables. The Rosenbrock's method of rotating coordinates has been used for solving the problem. Chan [29] has proposed an iterative technique by assuming initial value and then solving for a new value considering a small increment until the result converges. Jain *et al.* [30] have proposed a method in which the algebraic equation is solved for the initial value of and then the Secant method is used for the exact solution.

Suitability of pole changing (4/6 pole) of SEIG for harnessing more wind energy under wide variation in wind speed is presented in [31]. It is been concluded that at lower prime mover speed, the machine is to be operated with a higher number of poles (six) and at higher speed, it has to be operated with a lower number of poles (four) so as to reduce the excitation requirement over a large range of speed of the machine. Chan [32] has presented the steady state analysis and performance of SEIG driven by regulated and unregulated turbines. In case of regulated turbines for CSCF operation, per unit speed is determined directly by solving a quadratic equation. For

unregulated turbines, an additional iteration procedure using the Secant method has been used for dealing with the variable- speed nature of the turbine [33].

Alghuwainem [34] has examined the steady-state analysis and performance characteristics an isolated SEIG when a saturable reactor is connected across its terminals. The terminal voltage of a self-excited isolated induction generator, supplying a fixed load, may increase considerably due to a small increase in speed, excitation capacitance or both. Unregulated wind-turbines are often used due to their lower cost, in such cases the voltage may increase to a dangerously high level which may cause machine, load or capacitor damage. This detrimental effect can be overcome by connecting a saturable reactor across its terminals, the reactor tends to saturate at higher speeds and, thus, absorbs the excess reactive power supplied by the excitation capacitance, and limits the increase of the terminal voltage and improves the voltage regulation. The author [35] has also carried out the steady state analysis of standalone SEIG when a transformer is connected to its terminals to supply the load at different voltage levels or to step up the terminal voltage and obtained the desired improvement in voltage regulation. But the transformer introduces an additional nonlinearity, which complicates the analysis considerably. A technique has been suggested for formulating and solving the system's equation including the transformer saturation and the same technique is also applicable for nonlinear loads.

Sandhu *et al.* [36] have proposed an approach, which leads to a quadratic equation in slip making the steady-state analysis simple and comprehensive. Singh et al. [37] calculated the `capacitance requirement to maintain the terminal voltage constant under varying load and speed using loop impedance model and solved foe unknown variables capacitive reactance (X_c) and frequency (F) by Newton-Raphson method. Wang *et al.* [38] have presented an Eigen value-based approach to predict both minimum and maximum values of capacitance required for self-excitation of SEIG. Shridhar *et al* [39] presented the improvements in the performance of SEIG through series compensation using loop impedance model along with Newton-Raphson method to solve the unknown variables (X_m) and (F). Using the method of symmetrical components, a general analysis for three-phase SEIG with an asymmetrically connected load and excitation capacitance is presented in [40]. Kuo

et al. [41] had presented the analysis of isolated self-excited induction generator feeding a rectifier load.

Alolah *et al.* [42] have presented an optimization-based approach for the analysis of SEIG. The problem is formulated as a numerical optimization problem where no derivation of the analytical equation is needed. Instead of the step-by-step method analytical derivation, a global optimizer, such as those built in the mathematical software Matlab, is utilized to solve the total impedance or admittance equations of the circuit of the machine to obtain the frequency and other unknown parameters of the machine. Singh et al. [43] used the simulated annealing like approach to solve voltage regulation optimization problem. The solution obtained must satisfy the equality constraints on loop impendence (can be obtained by resolving equivalent loop impedance real and imaginary parts results into fourth and fifth degree polynomials of unknown variables (X_m) and (F) and using inequality constraints on generator and motor parameters and keeping the values of shunt and series capacitances within their specified upper and lower limits. Tarek Ahmed et al. [44] applied the loop impedance approach on the per phase approximated equivalent circuit of the SEIG with static VAr compensator. Two nonlinear simultaneous equation of the magnetizing reactance (X_m) are obtained manually by equating the imaginary and real parts to zero. Using these two equations, a 10th degree polynomial equation is derived and the frequency is determined.

Many researches from past few years had applied various artificial intelligent techniques for the Steady State Analysis of Self Excited Induction Generator [45-].

Genetic algorithm approach:

Joshi *et al*. [45] presented a new technique for the analysis of a three-phase self-excited induction generator feeding a three-phase balanced unity power factor load. A genetic algorithm has been proposed to find the generated frequency (F) and magnetizing reactance (X_m) simultaneously. The performance of the SEIG is greatly influenced by the operating speed, load, and excitation capacitance so proper handling of these parameters provides the required performance characteristics**.** Availability of the genetic algorithm (GA) a new and efficient technique for optimizing system behaviour provides an opportunity to predict the behaviour of the induction generator.

Sandhu *et al*. [46] proposed a genetic algorithm-based technique to identify these parameters to achieve constant voltage constant frequency operation for SEIG.

Kumaresan [47] made an approach employing genetic algorithm (GA) for the analysis of single-phase operation of three-phase self-excited induction generators. Using symmetrical components, the circuit equations have been written and an impedance matrix has been derived, which can be straightaway solved using this method. Apart from single-phase AC loads, feeding of DC loads through a controlled rectifier has also been considered and the analysis has been extended for this combined loading. Attia *et al*. [48] presented an application of the genetic algorithm (GA) for optimizing controller gains of the Self-Excited Induction Generator (SEIG) driven by the Wind Energy Conversion Scheme (WECS). GA calculates the optimum value for the gains of the variables based on the best dynamic performance and a domain search of the integral gains of the conventional controllers of the active and reactive control loop of the system. Velusami *et al*. [49] proposed the application of genetic algorithm to predetermine the steady state performance of single-phase SEIG with and without series compensation. Singh *et al*. [50] presents a genetic algorithm approach to determine steady-state modelling and the performance analysis of a six-phase SEIG for stand-alone renewable generation.

Fuzzy Logic approach:

Singaravelu *et al*. [51] had presented two mathematical models based on graph theory, and a fuzzy logic approach for the steady state analysis of three phase SEIG with and without series compensation. A Fuzzy Logic approach has been proposed to find the generated frequency (F) and magnetizing reactance (X_m) simultaneously in order to find the performance characteristics. Soliman *et al*. [52] presented an application of Fuzzy Logic Controller (FLC) to regulate the reactive-power of the Self Excited Induction Generator (SEIG) driven by Wind Energy Conversion Schemes (WECS). He introduced two types of controls, reactive-power control and active-power control which utilize the Fuzzy technique to enhance the overall dynamic performance and also observed the percentage overshoot, rising time and oscillation are improved by the fuzzy controller compared to that with PI controller type.

Palwalia *et al*. [53] presentd a digital design and implementation of a digital signal processor based fuzzy logic load controller to regulate the voltage and frequency of a three-phase self-excited induction generator through an equal time ratio control AC chopper controllable load that is suitable for a stand-alone power mode employing an unregulated turbine such as micro-hydro power generation.

1.2 OBJECTIVE OF THE THESIS

The objective of the present work is to obtain the steady state performance characteristics of Self Excited Induction Generator with and without series compensation using Fuzzy Logic. The simulation is to be carried out for given capacitances, prime mover speed and load. Also to experimentally validate the developed formulation.

1.4 ORGANIZATION OF THE THESIS

The thesis is organized into four chapters. The contents of these chapters are summarized as:

The Chapter 1 details the overview of SEIG, summary of literature review, objective of the thesis and organization of the thesis. The process of fuzzy logic, the mathematical modelling of SEIG based on graph theory and the application of the fuzzy logic process for steady state analysis of SEIG and the results obtained through the developed method for SEIG are presented in Chapter 2. In Chapter 3, the proposed method is applied for the analysis of compensated SEIG and the simulated performance characteristics for both short shunt SEIG and long shunt SEIG for various cases are also presented. The major conclusions and the scope of future work are presented in Chapter 4.

CHAPTER - 2

ANALYSIS OF SEIG USING FUZZY LOGIC

2.1 INTRODUCTION TO FUZZY LOGIC PROCESS

The entire real world is complex; it is found that the complexity arises from uncertainty in the form of ambiguity. According to Dr. Lotfi Zadeh, Principle of Compatibility, the complexity, and the imprecision are correlated and ads, "The closer one looks at a real world problem, the fuzzier becomes its solution [61].

The Fuzzy Logic is a mathematical tool for dealing with uncertainty. It provides a technique to deal with imprecision and information granularity. The fuzzy theory provides a mechanism for representing linguistic constructs such as "many," "low," "medium," "often," "few." In general, the fuzzy logic provides an inference structure that enables appropriate human reasoning capabilities. On the contrary, the traditional binary set theory describes crisp events, events that either do or do not occur. It uses probability theory to explain if an event will occur, measuring the chance with which a given event is expected to occur. Fuzzy logic is a superset of conventional Boolean logic that has been extended to handle the concept of partial truth-values between "completely true" and "completely false" , the theory of fuzzy logic is based upon the notion of relative graded membership and so are the functions of mentation and cognitive processes [61].

2.1.1 FUZZY SETS AND ITS PROPERTIES

Fuzzy sets have membership properties defined between 0 and 1. This means that if we take an attribute say 'red' we can express the colour of any particular apple as a position in this fuzzy set. We may say for example that it is 30% red and thus has a fuzzy truth value or membership function of 0.3. The relation of fuzzy truth value to actual values depends upon the desired mapping from the real world to the normalized range 0 to 1, and this is arbitrary.

Fuzzy sets support a flexible sense of membership of elements to a set. While in crisp set theory, an element either belongs to or does not belong to a set, in fuzzy

set theory many degrees of membership (between 0 and 1) are allowed. Thus a membership function $\mu_A(x)$ is associated with a fuzzy set Ã such that the function maps every element of the universe of discourse X (or the reference set) to the interval [0, 1], the membership can be written as $\mu_{\tilde{A}}(x) \rightarrow [0, 1]$

If X is a universe of discourse and x is a particular element of X, then a fuzzy set A defined on X may be written as a collection of ordered pairs

$$A=\{(x, \mu_{\tilde{A}}(x)),\ x \in X\} \quad (2.1)$$

Where, each pair $(x, \mu_{\tilde{A}}(x))$ is called a singleton. In crisp sets, $\mu_{\tilde{A}}(x)$ is dropped [62].

Membership Function

The membership function values need not always be described by discrete values. Quite often, these turn out to be as described by a continuous function. The membership function is a graphical representation of the magnitude of participation of each input. It associates a weighting with each of the inputs that are processed, define functional overlap between inputs, and ultimately determines an output response [63]. The fuzzy membership function for the fuzzy linguistic term "cool" relating to temperature may turn out to be as illustrated in Fig. 2.1 [62].

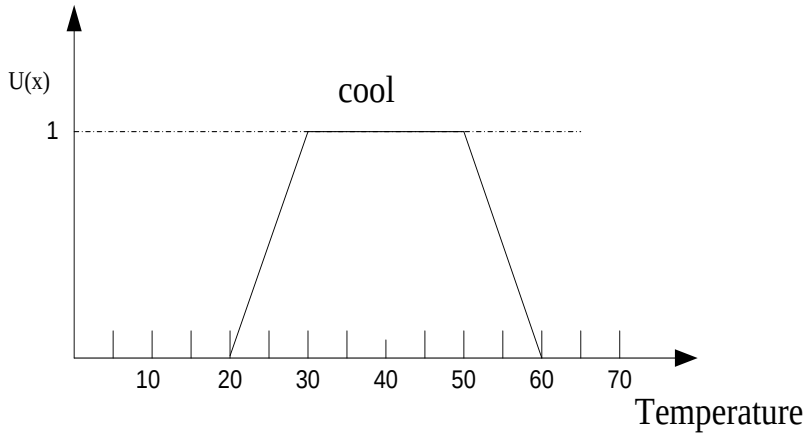

Fig. 2.1: Continuous membership function for "cool"

A membership function can also be given mathematically as

$$\mu_{\tilde{A}}(x) = \frac{1}{(1+x)^2} \qquad (2.2)$$

The graph is as shown in Fig. 2.2

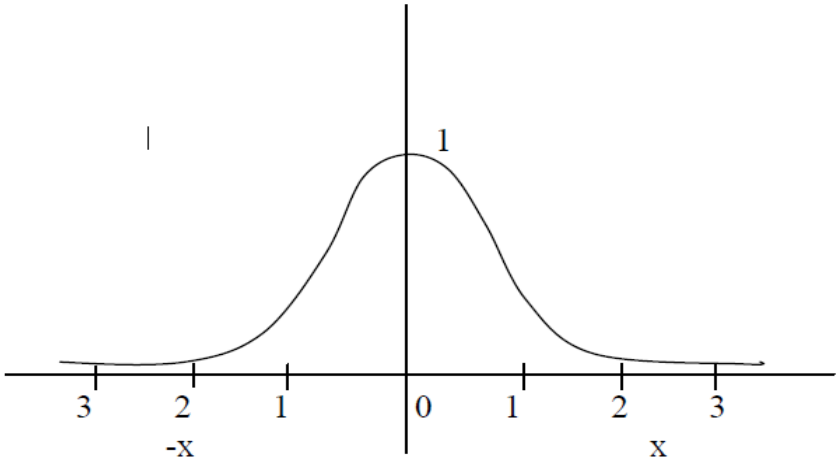

Fig. 2.2: Continuous membership function dictated by a mathematical function

Different shapes of membership functions exit. The commonly used shape to describe the membership function is triangular, but bell, trapezoidal and exponential can also be used as shown in Fig. 2.3 with their variation.

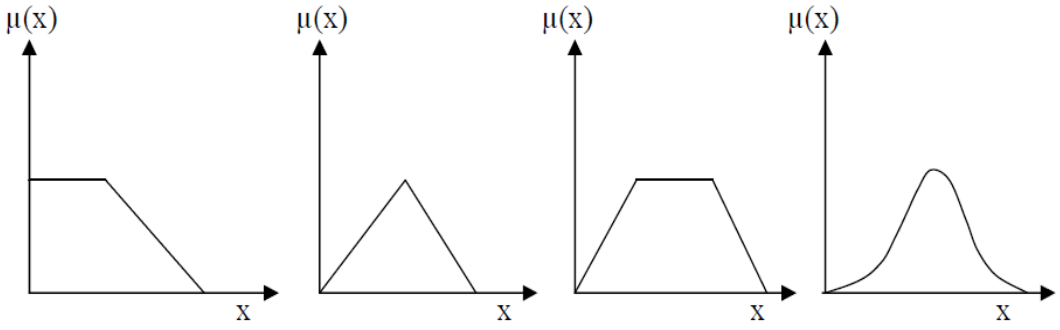

Fig. 2.3: Different shapes of membership function graphs

Rules associate ideas and relate one event to another [64]. Fuzzy machines, which always tend to mimic the behaviour of man, also work in the same way. However, the decision and the means of choosing that decision are replaced by fuzzy sets and the rules are replaced by fuzzy rules. Fuzzy rules also operate using a series of if-then statements. For instance, if X is positive then A, and if Y is negative then B,

where A and B are all sets of X and Y. Fuzzy rules define fuzzy patches, which is the key idea in fuzzy logic.

Basic Fuzzy Set Operations

Given X to be the universe of discourse and $\tilde{A}$ and $\tilde{B}$ to be fuzzy sets with $\mu_{\tilde{A}}(x)$ and $\mu_{\tilde{B}}(x)$ as their respective membership functions, the basic fuzzy set operations are as follows:

Union: The union of two fuzzy sets $\tilde{A}$ and $\tilde{B}$ is a new fuzzy set $\tilde{A} \cup \tilde{B}$ also on X with a membership function defined as

$$\mu_{\tilde{A}\cup\tilde{B}}(x) = \max\left(\mu_{\tilde{A}}(x), \mu_{\tilde{B}}(x)\right) \tag{2.3}$$

Intersection: The intersection of fuzzy sets $\tilde{A}$ and $\tilde{B}$ is a new fuzzy set $\tilde{A} \cap \tilde{B}$ with membership function defined as

$$\mu_{\tilde{A}\cap\tilde{B}}(x) = \min\left(\mu_{\tilde{A}}(x), \mu_{\tilde{B}}(x)\right) \tag{2.4}$$

Complement: The complement of a fuzzy set $\tilde{A}$ is a new fuzzy set $\overline{\tilde{A}}$ with a membership function defined as

$$\mu_{\tilde{A}}(x) = 1 - \mu_{\tilde{A}}(x) \tag{2.5}$$

Properties of Fuzzy Sets

Fuzzy sets follow the same properties as crisp sets. In fact, crisp sets can be thought of as special instances of fuzzy sets. Any fuzzy set $\tilde{A}$ is a subset of the reference set X. Also, the membership of any element belonging to the null set $\emptyset$ is 0 and the membership of any element belonging to the reference set 1. Frequently used properties of fuzzy sets are listed below [65]

Commutativity:
$$\tilde{A} \cup \tilde{B} = \tilde{B} \cup \tilde{A}$$
$$\tilde{A} \cap \tilde{B} = \tilde{B} \cap \tilde{A} \tag{2.6}$$

Associativity:
$$\tilde{A} \cup \left(\tilde{B} \cup \tilde{C}\right) = (\tilde{A} \cup \tilde{B}) \cup \tilde{C}$$
$$\tilde{A} \cap \left(\tilde{B} \cap \tilde{C}\right) = (\tilde{A} \cap \tilde{B}) \cap \tilde{C} \tag{2.7}$$

Distributivity:
$$\tilde{A} \cup \left(\tilde{B} \cap \tilde{C}\right) = \left(\tilde{A} \cup \tilde{B}\right) \cap (\tilde{A} \cup \tilde{C})$$
$$\tilde{A} \cap \left(\tilde{B} \cup \tilde{C}\right) = \left(\tilde{A} \cap \tilde{B}\right) \cup (\tilde{A} \cap \tilde{C}) \tag{2.8}$$

Idempotence:
$$\tilde{A} \cup \tilde{A} = \tilde{A} \text{ and } \tilde{A} \cap \tilde{A} = \tilde{A} \tag{2.9}$$

Identity:
$$\tilde{A} \cup \emptyset = \tilde{A} \text{ and } \tilde{A} \cap X = \tilde{A}$$
$$\tilde{A} \cap \emptyset = \tilde{A} \text{ and } \tilde{A} \cup X = X \tag{2.10}$$

Transitivity: If $\tilde{A} \subseteq \tilde{B}$ and $\tilde{B} \subseteq \tilde{C}$, then $\tilde{A} \subseteq \tilde{C}$ (2.11)

Involution: $\overline{\bar{\tilde{A}}} = \tilde{A}$ (2.12)

De Morgan's Laws: $\overline{(\tilde{A} \cap \tilde{B})} = (\bar{\tilde{A}} \cup \bar{\tilde{B}})$

$\overline{(\tilde{A} \cup \tilde{B})} = (\bar{\tilde{A}} \cap \bar{\tilde{B}})$ (2.13)

Since fuzzy sets can overlap, the laws of excluded middle do hold good. Thus,

$\tilde{A} \cup \bar{\tilde{A}} \neq X$ (2.14)

$\tilde{A} \cup \bar{\tilde{A}} \neq \emptyset$ (2.15)

2.1.2 FUZZY LOGIC

Fuzzy logic is reasoning with fuzzy sets. Unlike crisp logic, truth values of fuzzy logic are multi-valued such as absolutely true, absolutely false, very true and so on and are numerically equivalent to (0-1). A statement which acquires a fuzzy truth value is called a 'fuzzy proposition'. Thus, given $\tilde{P}$ to be a fuzzy proposition, $T(\tilde{P})$ represents the truth value attached to $\tilde{P}$ [62]. The fuzzy set operations given by equations 2.3, 2.4, 2.5 also valid for a given fuzzy propositions say, $\tilde{P}$, $\tilde{Q}$ and their truth values $T(\tilde{P})$, $T(\tilde{Q})$.

Fuzzy Inference

The ultimate goal of fuzzy logic is to form the theoretical foundation for reasoning about imprecise propositions; such reasoning has been referred to as approximate reasoning [5, 6]. Approximate reasoning is analogous to classical logic for reasoning with precise propositions, and hence is an extension of classical propositional calculus that deals with partial truths.

Suppose we have a rule-based format to represent fuzzy information. These rules are expressed in conventional antecedent-consequent form, such as

- Generalized Modus Pones (GMP)
- Generalized Modes Tollens (GMT)

The GMP is formally stated as

IF x is $\tilde{A}$ THEN y is $\tilde{B}$

x is $\tilde{A}'$

---

y is $\tilde{B}'$ (2.16)

where, $\tilde{A}, \tilde{B}$, $\tilde{A}'$ and $\tilde{B}'$ are fuzzy terms. Every fuzzy linguistic statement above the line is analytically known and below the line is analytically unknown.

To compute the membership function of $\tilde{B}'$, the max-min composition of fuzzy set $\tilde{A}'$ with $\tilde{R}(x, y)$ which is the known implication relation (IF-THEN relation) is used. That is,

$$\tilde{B}' = \tilde{A}' \circ \tilde{R}(x, y) \quad (2.17)$$

In terms of membership function,

$$\mu_{\tilde{B}'}(y) = \max\left(\min\left(\mu_{\tilde{A}'}(x), \mu_{\tilde{R}}(x, y)\right)\right) \quad (2.18)$$

where $\mu_{\tilde{A}'}(x)$ is the membership function of $\tilde{A}'$, $\mu_{\tilde{R}}(x, y)$ is the membership function of the implication and $\mu_{\tilde{B}'}(y)$ is the membership function of $\tilde{B}'$.

And, GMT has the form

IF x is $\tilde{A}$ THEN y is $\tilde{B}$

y is $\tilde{B}$

---

x is $\tilde{A}'$ (2.19)

The membership of $\tilde{A}'$ is computed on similar lines as

$$\tilde{A}' = \tilde{B}' \circ \tilde{R}(x, y) \quad (2.20)$$

In terms of membership function,

$$\mu_{\tilde{A}'}(y) = \max\left(\min\left(\mu_{\tilde{B}'}(x), \mu_{\tilde{R}}(x, y)\right)\right) \quad (2.21)$$

Process of Fuzzy Logic

The main structure of the proposed fuzzy logic process shown in Fig. 2.4 comprises four principal components: a fuzzification interface, a rule base, process logic and a defuzzification interface [69] they are briefed here with as,

Fuzzification:

Fuzzification is the process of making a crisp (G) quantity fuzzy (G_{fuz}).They carry considerable uncertainty. If the form of uncertainty happens to arise because of imprecision, ambiguity, or vagueness, then the variable is probably fuzzy and can be represented by a membership function. Simply, under fuzzification, the membership functions defined on the input variables are applied to their actual values, to determine the degree of truth for each rule premise.

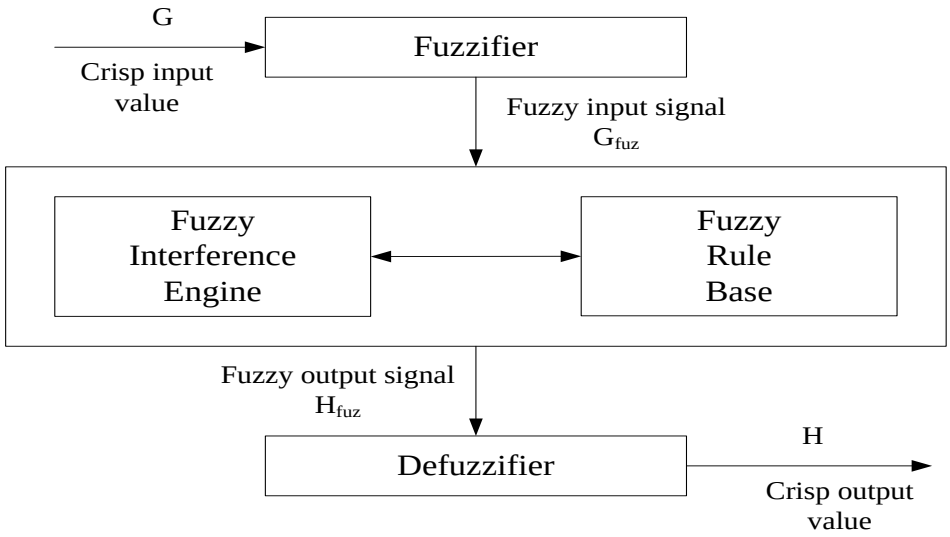

Fig. 2.4: Fuzzy Logic Process

Fuzzy Rule Base:

In the field of artificial intelligence (machine intelligence) there are various ways to represent knowledge. Perhaps the most common way to represent human knowledge is to form it into natural language expressions of the type

IF premise (antecedent), THEN conclusion (consequent) (2.22)

The above form in 2.22 is commonly referred to as the IF–THEN rule-based form; this form generally is referred to as the deductive form. It typically expresses that IF (a set of conditions) are satisfied THEN (a set of consequents) can be inferred.
This form of knowledge representation, characterized as shallow knowledge.

By using the basic properties and operations defined for fuzzy sets, any compound rule structure may be decomposed and reduced to a number of simple canonical rules given as,

Table 2.1: The canonical form for a fuzzy rule base

Rule 1:	IF condition C_1, THEN restriction R_1
Rule 2:	IF condition C_2, THEN restriction R_2
⋮	
Rule r:	IF condition C_r, THEN restriction R_r

These rules are based on natural language representations and models, which are themselves based on fuzzy sets and fuzzy logic. The fuzzy level of understanding and describing a complex system is expressed in the form of a set of restrictions on the output based on certain conditions of the input (see Table 2.1). Restrictions are generally modelled by fuzzy sets and relations. These restriction statements are usually connected by linguistic connectives such as ‘‘and,’’ ‘‘or,’’ or ‘‘else.’’ The restrictions$R_1, R_2, \ldots, R_r$ apply to the output actions, or consequents of the rules [5]. For the defined rule base the logic has been implemented from the fuzzy inference procedure i.e. GMP or GMT, the fuzzy output signal is generated (H_{fuz}).

Defuzzification:

The output of a fuzzy process needs to be a single scalar quantity as opposed to a fuzzy set. Defuzzification is the conversion of a fuzzy quantity (H_{fuz}).to a crisp output value (H), just as fuzzification is the conversion of a crisp quantity to a fuzzy quantity. The output of a fuzzy process can be the logical union of two or more fuzzy membership functions defined on the universe of discourse of the output variable [5].

$$H_{fuz_k} = \bigcup_{i=1}^{k} H_{fuz_i} = H_{fuz} \tag{2.23}$$

There are many methods that have been proposed in the literature in recent years [8], namely max-membership method, centre of sums method, centriod method, mean of

max method etc. but centroid method is popular and has been used and therefore is briefed here with as,

***Centroid method**:*

This procedure (also called centre of area, centre of gravity) is the most prevalent and physically appealing of all the defuzzification methods; it obtains the centre of area (H) occupied by the fuzzy set (H_{fuz}). It is given by the algebraic expression

$$H = \frac{\int \mu(H_{fuz})\, H_{fuz}\, dH_{fuz}}{\int \mu(H_{fuz})\, dH_{fuz}} \tag{2.24}$$

for a continuous membership function, and

$$H = \frac{\sum_{i=1}^{n} H_{fuz_i} \mu\left(H_{fuz_i}\right)}{\sum_{i=1}^{n} \mu\left(H_{fuz_i}\right)} \tag{2.25}$$

for a discrete membership function.

Here, n represents the number of variables in sample, $H_{fuz_i}{}'s$ are the variables, and $\mu\left(H_{fuz_i}\right)$ is its membership function.

2.2 FUZZY LOGIC APPROACH FOR STEADY ANALYSIS OF SEIG

Self excitation in an induction machine occurs when the rotor is driven by a prime mover and a suitable capacitance is connected across the stator terminals. The machine operating in this mode is called a self-excited induction generator (SEIG) which has been increasingly utilized in stand-alone generation systems that employ wind or hydro power. Unlike induction generators connected to the power utility grid, both the frequency and the magnetizing reactance (which depends upon magnetic saturation) of the SEIG vary with load even when the rotor speed is maintained constant. Therefore, a crucial step in the steady-state analysis of the SEIG is, given the machine parameters, speed**,** excitation capacitance and load impedance, to determine the value of the per-unit frequency (F) and the magnetizing reactance (X_m), which result in exact balance of active and reactive power across the air gap [29].

Many researchers have tackled this problem in the past few decades and developed different solution techniques based on the steady-state equivalent circuit. Most of the methods available in literature [18-44] on steady state performance evaluation of a SEIG need manual separation of real and imaginary component of complex impedance to derive the specific model and applications of Newton-Raphson method or unconstrained nonlinear optimization method [54-57]. It is also observed that the mathematical model is not the same for different types of loads, and capacitor connections configuration at the machine terminals. Subsequently the coefficients of mathematical model are also bound to change with change in load and capacitance configuration at the machine terminals. The major difficulty in applying the Newton- Raphson method is the need to establish the Jacobian matrix which involves lengthy mathematical derivations, and partial differentiation, and inverse of Jacobian matrix to obtain solution. Unconstrained nonlinear optimization techniques such as Rosenbrock's method (gradient method) [54] and Hooke and Jeeves method (pattern search method) generally involve more number of function evaluation over the practical range of load impendence [55-57].

In the present work, new mathematical models are presented using loop impedance methods based on graph theory [51]. The mathematical models developed using graph theory completely avoids the tedious manual work involved in segregating the real and imaginary components of the complex impedance of the equivalent circuit. Next, to carry out the steady state analysis of SEIG a fuzzy logic approach is used instead of classical Newton-Raphson method [18] or unconstrained nonlinear optimization method [54-57]. In the present work, analysis was carried out using fuzzy logic process with a simple rule base having seven rules tallying with seven linguistic variables which involve only simple logical operations and relatively simple programming [51]. Though the fuzzy rules are simple, their performances are sufficiently found to be robust [67] which is validated by comparing the simulated results with the experimentally obtained results. The developed fuzzy logic processing uses general mathematical model of SEIG and the same model can be implemented for any type of load.

2.2.1 STEADY STATE MODELLING OF SEIG

The formulation of a suitable mathematical model is the first step in the analysis of a three phase SEIG. The model must describe the characteristics of individual components of three phase SEIG as well as the relations that govern the interconnection of these elements. In the modelling and analysis of three phase SEIG presented here, the following assumptions have been made [19]

- Only the magnetizing reactance is assumed to be affected by magnetic saturation, and all other parameters of the equivalent circuit are assumed to be constant. Self excitation results in the saturation of the main flux. As the value of the magnetizing reactance X_M reflects the magnitude of the main flux, it is essential to incorporate in the analysis the variation of X_M with the saturation level of the main flux. Passage of the leakage fluxes occurs primarily in the air and thus these fluxes are not affected to any large extent by the saturation of the main flux.
- Leakage reactance of stator and rotor, in per unit, are taken to be equal.
- Core loss in the machine is neglected.
- MMF space harmonics and time harmonics in the induced voltage and current waveforms are ignored. This assumption is valid in well designed machines.

2.2.2.1 Equivalent circuit of the SEIG

The steady state equivalent circuit of a capacitor self excited induction generator with a resistance-inductance (R) load connected at terminals is shown in Fig. 2.5

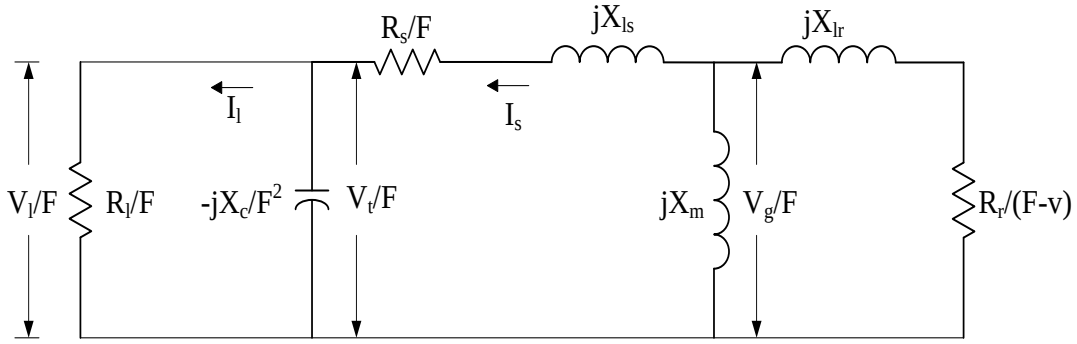

Fig. 2.5: Equivalent circuit of the SEIG

where:

R_s, R_r = per phase stator and rotor (referred to stator) resistance

R_l = per phase load resistance

X_{ls}, X_{lr} = per phase stator and rotor (referred to stator) leakage reactance

X_m = magnetising reactance

X_c = per phase capacitive reactance of the terminal capacitor *C*

(all reactances referred to above relate to the base frequency F)

F, ϑ = p.u. frequency and speed

I_s, I_r = per phase stator and rotor (referred to stator) current

I_l = per phase load current

V_t = terminal and air gap voltage

V_g = air gap voltage

V_l = per phase load voltage, respectively.

The various elements of equivalent circuit can be represented as given below.

$$Z_M = jX_m; \qquad Z_{RR} = {R_r}/{(F - \vartheta)} + jX_{lr};$$

$$Z_S = {R_s}/{F} + jR_{ls}; \qquad Z_C = {-jX_c}/{F^2} \quad \text{and}$$

$$Z_L = {R_l}/{F}$$

2.2.2.2 Use of graph theory

In this thesis a new mathematical model based on graph theory is developed using loop impedance method for the steady state analysis of three phase SEIG from equivalent circuit of generator shown in Fig. 2.5. The developed models result in a matrix form provides convenience for computer solutions.

If in the equivalent circuit of the SEIG all the elements such as resistors, inductors, capacitors, etc., are replaced by lines with dots at both ends, then the equivalent circuit becomes the graph of the equivalent circuit as shown in Fig. 2.6. Graph of an equivalent circuit is drawn by keeping all points of intersection of two or

more branches known as nodes and representing the equivalent circuit elements by lines, voltage and current sources by their internal impedance. Number 1, 2, etc., may be given to identify the elements and letters A, B, etc., may be given to denote the nodes. If directions or orientations are shown in the graph, then it is known as an oriented graph. Orientations may be given arbitrarily.

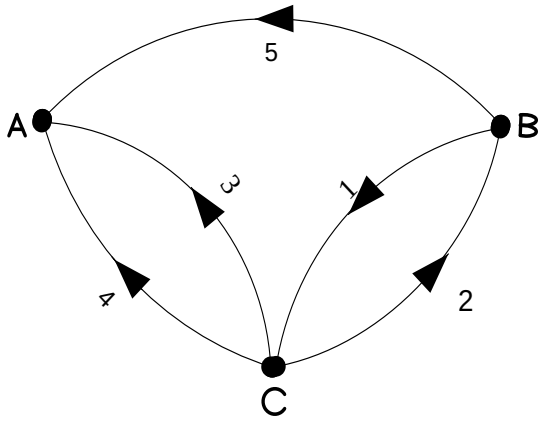

Fig. 2.6: Graph with nodes

For the steady state equivalent circuit (Fig. 2.5) based on loop impedance method using graph theory, the graph with links, trees can be formed as shown in Fig. 2.7. The number of branches, nodes, tree branches and links of the graph of the Fig. 2.7 is as follows:

Number of branches (B) = 5, Number of Nodes (N) = 3

Number of Tree branches = N-1= 2, and Number of Links= B-N + 1 = 3

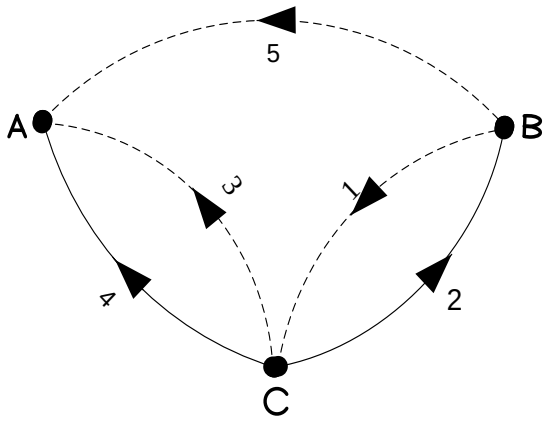

Fig. 2.7: Tree with Links

The tie set matrix can be formed for the graph as shown in Fig.2.7 as in Table 2.2

Table 2.2 – Tie Set Matrix

Link or Loop Current	Branches				
	1	2	3	4	5
i_1	1	1	0	0	0
i_3	0	0	1	-1	0
i_5	0	1	0	-1	1

The equilibrium equation in matrix form on loop basis can be expressed as [63].

$$\{[M][Z_b][M]^T\}\,[I] = [M]\,\{[V_s] - [Z_b][I_s]\} \qquad (2.26)$$

In Fig. 2.5 there is no current and voltage sources, therefore, [Vs]=0 and [Is]=0 in (2.26) and hence the equilibrium equation (2.26) is reduced to (2.27)

$$\{[M][Z_b][M]^T\}\,[I] = 0 \qquad (2.27)$$

Where,

$[M]$ is the tie-set matrix, $[M]^T$ is the transposed tie-set matrix,

$[Z_b]$ is the branch-impedance matrix, $[I]$ is the independent loop current column matrix.

The matrices [M], $[Z_b]$ and $[I]$ are expressed as

$$[M] = \begin{bmatrix} 1 & 1 & 0 & 0 & 0 \\ 0 & 0 & 1 & -1 & 0 \\ 0 & 1 & 0 & -1 & 1 \end{bmatrix}, \qquad [M]^T = \begin{bmatrix} 1 & 0 & 0 \\ 1 & 0 & 1 \\ 0 & 1 & 0 \\ 0 & -1 & -1 \\ 0 & 0 & 0 \end{bmatrix}$$

$$[Z_b] = \mathrm{diag}\{Z_M, Z_{RR}, Z_C, Z_L, Z_S\}, \text{ and } [I] = [i_1 \;\; i_3 \;\; i_5]^T$$

By substituting [M], $[M]^T$, $[Z_b]$ and $[I]$ in (2.27), after simplification the following matrix equation is obtained.

$$\begin{bmatrix} Z_M + Z_{RR} & 0 & Z_{RR} \\ 0 & Z_C + Z_L & Z_L \\ Z_{RR} & Z_L & Z_{RR} + Z_L + Z_S \end{bmatrix} \begin{bmatrix} i_1 \\ i_3 \\ i_5 \end{bmatrix} = \begin{bmatrix} 0 \\ 0 \\ 0 \end{bmatrix} \quad (2.28)$$

The above equation (2.28) can be written as

$$[Z]\,[I] = [0] \quad (2.29)$$

where,

$$[Z] = \{[M][Z_b][M]^T\}\,.$$

Therefore, from the equivalent circuit of SEIG and by graph theory approach using loop impedance method the equilibrium equation essential for obtaining the performance characteristics of SEIG is given in eqn. (2.29).

2.2.2 STEADY STATE ANALYSIS

If an appropriate three-phase capacitor bank is connected across an externally driven induction machine, an EMF is induced in the machine winding due to the excitation provided by the capacitor. As the voltage builds up, the resulting air gap flux drives the machine into saturation, which gradually decreases the saturated magnetising reactance to a value that results in root of eqn. (2.29) being reduced to zero. This signifies the steady-state condition being reached, and this saturated value of det [Z] has to be used in the steady-state analysis. Therefore, in Fig. 2.5, both the steady-state values of X_m and F are unknown and have to be determined for the given capacitance, speed and load, to calculate the steady-state response using the equivalent circuit.

Under steady state self excitation $[I] \neq 0$ and therefore from above eqn. 2.29 $[Z]$ should be a singular matrix i.e., det $[Z] = 0$. It implies that both the real and the imaginary components of det $[Z]$ should be independently zero, i.e., if det $[Z] = a + j$ then real quantity a=0 and the imaginary quantity b=0.Therefore to obtain unknown variables which result det $[Z]$=0, a fuzzy logic process based approach has been adopted.

As explained earlier, the main structure of the proposed fuzzy logic process comprises four principal components: a fuzzification interface, a rule base, process logic and a defuzzification interface.

The fuzzification interface involves the following function.

- By calculating det [Z] the real quantity G_a and imaginary quantity G_b are obtained.
- The parameters G is elected as crisp input value for the fuzzy logic process. The maximum (or worst) parameter (G_{amax} or G_{bmax}) determines the range of scale of mapping that transfers input values into corresponding universe of discourse at every iteration.
- The input signals G is fuzzified into fuzzy signals (G_{afuz} or G_{bfuz}) with seven linguistic variables: large negative (LN), medium negative (MN), small negative (SN), zero (ZR), small positive (SP), medium positive (MP), large positive (LP). They are represented in triangular function.
- Fig. 2.8 gives sketches of these membership functions. Each three points (left bottom, top, right bottom)is designed as

$$\text{LN: } \left[-\infty, -G_{max,}\ {}^{-G_{max}}/_{3.0}\right], \qquad \text{MN: } \left[-G_{max}, {}^{-G_{max}}/_{2.0}, 0.0\right],$$

$$\text{SN: } \left[{}^{-G_{max}}/_{3.0}, {}^{-G_{max}}/_{6.0}, 0.0\right], \quad \text{ZR: } \left[{}^{-G_{max}}/_{12.0}, 0.0, {}^{G_{max}}/_{12.0}\right],$$

$$\text{SP: } \left[0.0, {}^{G_{max}}/_{6.0}, {}^{G_{max}}/_{3.0}\right], \qquad \text{MP: } \left[0.0, {}^{G_{max}}/_{2.0}, G_{max}\right], \text{ and}$$

$$\text{LP: } \left[{}^{-G_{max}}/_{3.0}, G_{max}, \infty\right],$$

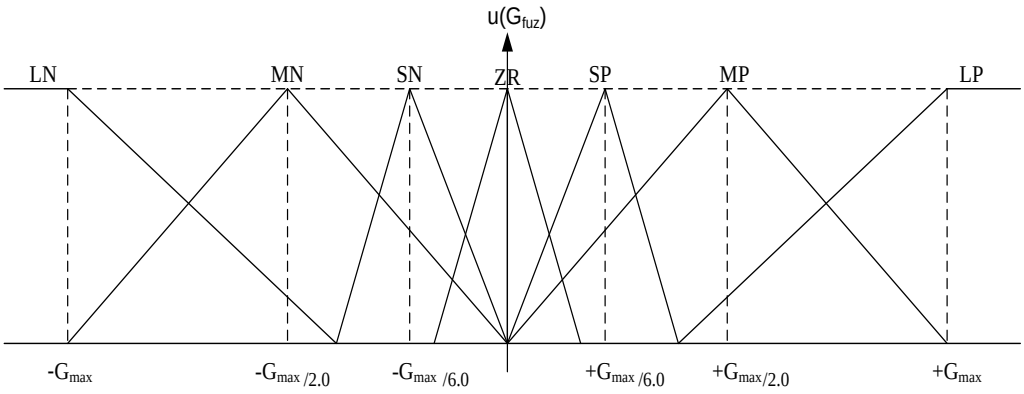

Fig. 2.8: Membership function for input signals G_{fuz}

The Rule base involves seven rules tallying with seven linguistic variables:

Rule 1: if G_{fuz} is LN then H_{fuz} is LN,

Rule 2: if G_{fuz} is MN then H_{fuz} is MN,

Rule 3: if G_{fuz} is SN then H_{fuz} is SN,

Rule 4: if G_{fuz} is ZR then H_{fuz} is ZR,

Rule 5: if G_{fuz} is SP then H_{fuz} is SP,

Rule 6: if G_{fuz} is MP then H_{fuz} is MP, and

Rule 7: if G_{fuz} is LP then H_{fuz} is LP

The fuzzy input signals G_{fuz} is sent to process logic, which generates the fuzzy output signals H_{fuz} based on the previous rule base and are represented by seven linguistic variables similar to input fuzzy signals.

The output fuzzy signals H_{fuz} are then sent to the defuzzification interface, which performs the following functions:

- The maximum corrective action H_{amax} or H_{bmax} of unknown variables determines the range of scale mapping that transfers the output signals into the corresponding universe of discourse at every iteration. Therefore, each three points (left bottom, top, right bottom) of the triangular membership functions H_{fuz} is designed in similar way to Fig. 2.8.

  LN: $\left[-\infty, -H_{max,}\ {}^{-H_{max}}/_{3.0}\right]$, MN: $\left[-H_{max},\ {}^{-H_{max}}/_{2.0}, 0.0\right]$,

  SN: $\left[{}^{-H_{max}}/_{3.0}, {}^{-H_{max}}/_{6.0}, 0.0\right]$, ZR: $\left[{}^{-H_{max}}/_{12.0}, 0.0, {}^{H_{max}}/_{12.0}\right]$,

  SP: $\left[0.0, {}^{H_{max}}/_{6.0}, {}^{H_{max}}/_{3.0}\right]$, MP: $\left[0.0, {}^{H_{max}}/_{2.0}, H_{max}\right]$,and

  LP: $\left[{}^{-H_{max}}/_{3.0}, H_{max}, \infty\right]$,

- Finally the defuzzifier will transform fuzzy output signals H_{fuz} intro crisp values H. The centroid-of-area (COA) defuzzification strategy [5] is adapted.

The number of triangular fuzzy-membership functions used in the present work and fuzzy rules are selected heuristically to minimize number of iterations required for convergence.

The above mentioned fuzzy logic process generate the correction to the unknown variables i.e, the incremental values of X_m is ΔX_m and F is ΔF, and they are updated in matrix Z and again det [Z] is evaluated , until det [Z] reach desired tolerance value ε (0.0001). Having obtained the desired tolerance value the iteration is terminated and results unknown variables i.e., the frequency (F) and saturated value of magnetising reactance (X_m) for given value of capacitance(C), speed (ϑ) and load(R_l). Using X_m and F, air gap voltage (V_g) can be found from the magnetisation curve (plot of V_g/F v/s X_m). Knowing the F, X_m and V_g/F, the equivalent circuit is solved and the steady state performance parameters are calculated using the equations as follows,

$$I_s = \frac{\frac{V_g}{F}}{\frac{R_s}{F} + jX_{ls} - \frac{jX_c R_l}{F^2 R_l - jX_c F}} \tag{2.30}$$

$$I_r = \frac{\frac{-V_g}{F}}{\frac{R_r}{F-\vartheta} + jX_{lr}} \tag{2.31}$$

$$I_l = \frac{-jX_c I_s}{R_l - jX_c} \tag{2.32}$$

$$V_t = I_l R_l \tag{2.33}$$

$$\text{input power, } P_{in} = \frac{-3|I_r{}^2|R_r F}{F-\vartheta} \tag{2.34}$$

$$\text{output power, } P_{out} = 3|I_l{}^2|R_l \tag{2.35}$$

2.2.3 Algorithm and Flow chart of Fuzzy Logic

The flow chart of Fuzzy Logic Process based computational algorithm for solution of X_m, F and steady state performance of SEIG is shown in Fig. 2.9 and the algorithm is given as -

Step 1: Read all required parameters for matrix[Z].

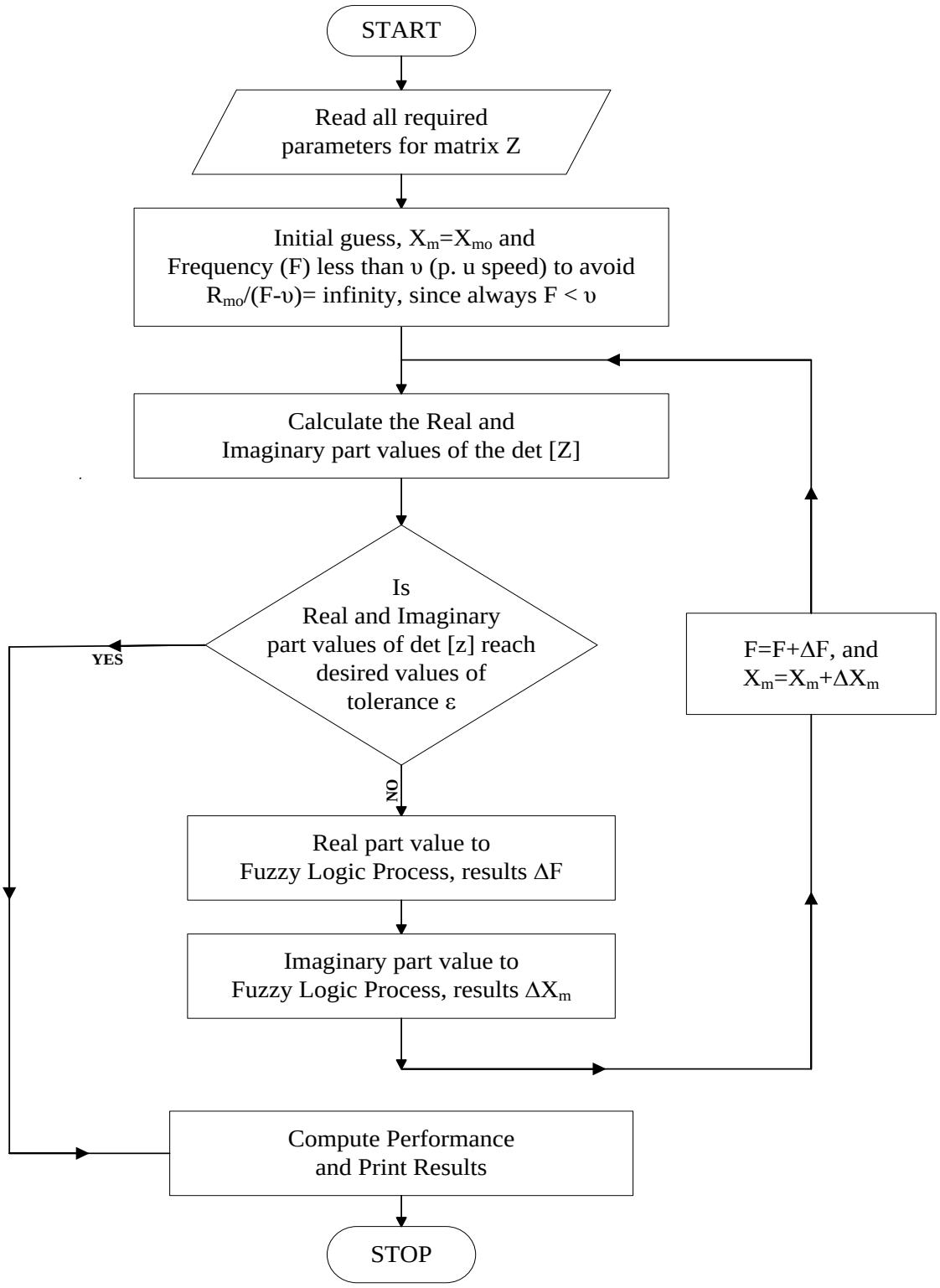

Fig. 2.9: Flow chart of Fuzzy Logic algorithm

Step 2: Assume initial values, $X_m = X_{mo}$ and F= 0.99 ϑ to avoid $R_r/(F - \vartheta) = \infty$, and motoring arrangement.

Step 3: Calculate the real and imaginary part values of the det $[Z]$. Set iteration count, itr =1.

Step 4: Check whether real and imaginary part values of det $[Z]$ reach desired value of tolerance ε, if yes go to step 8 otherwise go to step 5.

Step 5: The real part value of det $[Z]$ is introduced to the 'fuzzy logic process' as explained earlier, which results in the incremental change in frequency ΔF.

Step 6: The imaginary part value of det $[Z]$ is introduced to the 'fuzzy logic process' as explained earlier, which results in the incremental change in magnetising reactance ΔX_m.

Step 7: Update the values of frequency (F) and magnetising reactance (X_m) as $F=F+\Delta F$ and $X_m = X_m + \Delta X_m$, Increment the iteration count itr = itr +1 and go to step 3.

Step 8: Compute the performance parameters of the machine using equations (2.30 - 2.35) and print the results.

2.3 RESULTS AND DISCUSSION

In this section the performance has been simulated for the given machines, Machine: 1 having data as 4-pole, 50Hz delta connected stator winding rated 230V, 12.5A and 5hp and Machine: 2 having data 50Hz delta connected stator winding rated 415V, 10.1A, 5.5 kW and 5hp. The results of machine 2 are experimentally validated for 1.0 p.u speed. The specifications of the machines are given in Appendix.

2.3.1 PERFORMANCE FOR GIVEN CAPACITANCE

The performance characteristics have been plotted for the above given machines for a fixed value of shunt capacitance (C). The simulated characteristics are shown in Fig. 2.10 for machine 1 and Fig. 2.11 for machine 2.

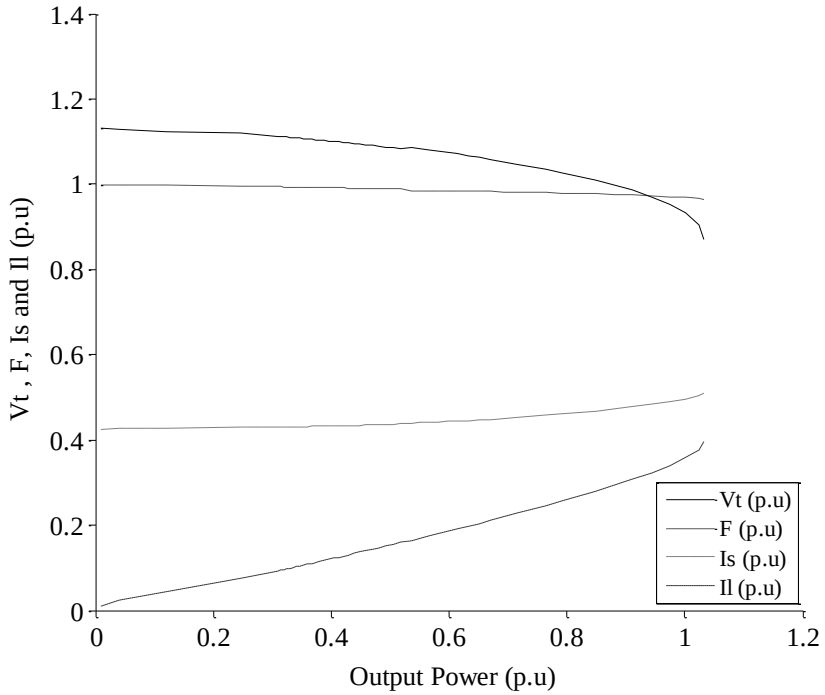

Fig. 2.10: Typical Characteristics of SEIG at 38µF (machine 1)

Fig. 2.10 shows the variations of terminal voltage (V_t), frequency (F), stator current (I_s) and load current (I_l) with output power for a given capacitance, C=38μF, X_c=2.628 p.u.

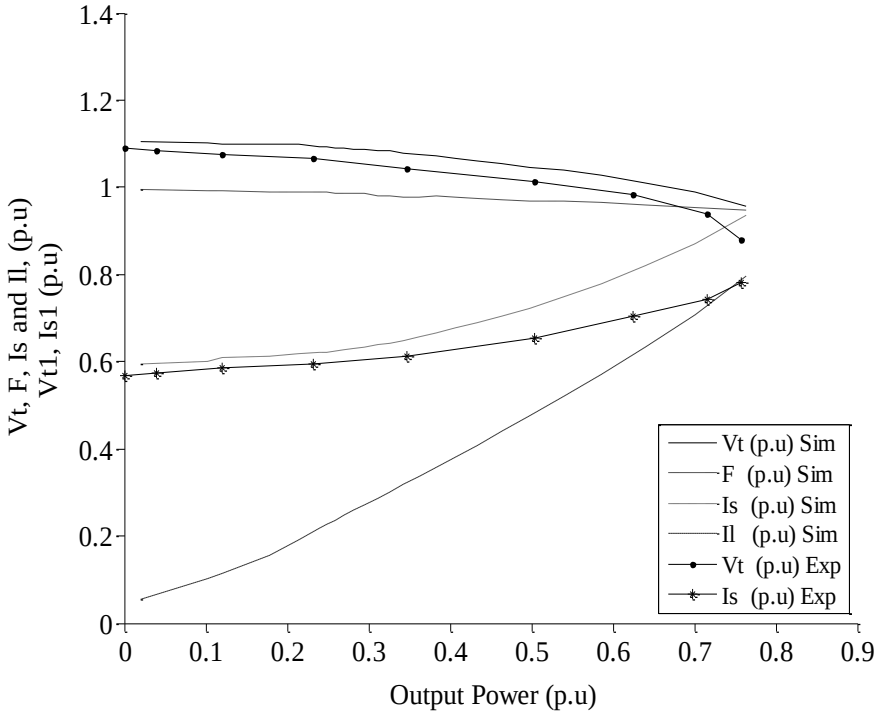

Fig. 2.11: Typical Characteristics of SEIG at 24 µF (machine 2)

Fig. 2.11 shows the variations of terminal voltage (V_t), frequency (F), stator current (I_s) and load current (I_l) with output power for machine 2 at a given capacitance, C=24 μF, X_c=1.8635 p.u.

As clear from Fig. 2.11, the terminal voltage decreases and stator current increases with the loading, the frequency varies only in 4 % band. After loading of about 0.8 p.u, any attempt to have large output results into voltage collapse due to machine operates in unsaturated regions.

2.3.2 EFFECT OF VARIATION OF CAPACITANCE

The variation in value of terminal capacitance affects the output characteristics of an SEIG. For different value of excitation capacitance, C=32.5μF, X_c= 3.066 p.u; C=38 μF, X_c=2.628 p.u; C=43.5 μF, X_c= 2.299 p.u. at the speed of 1.0 p.u results into the characteristics for machine 1 as shown in Fig. 2.12.

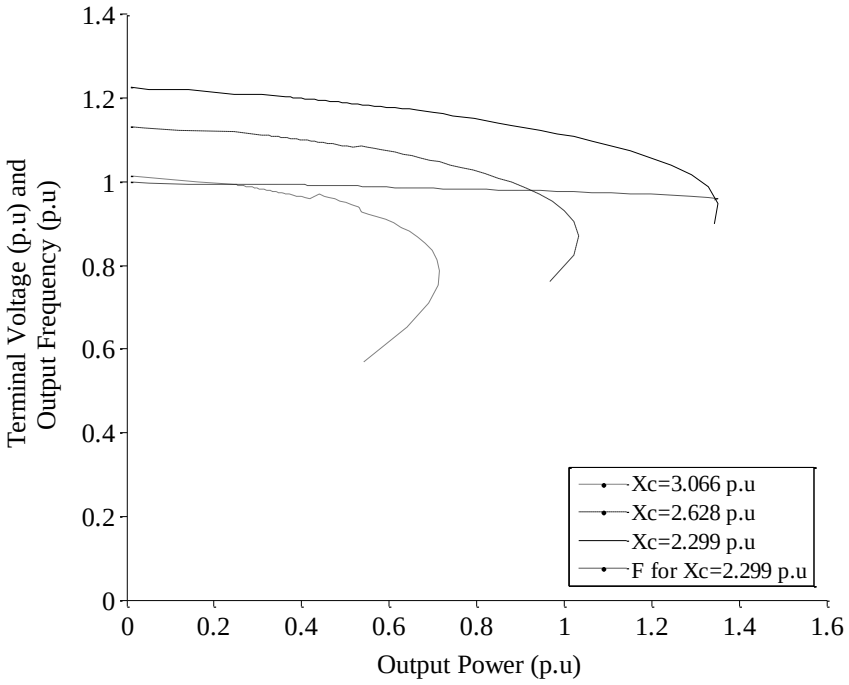

Fig. 2.12 (a): Load Characteristics for different values of capacitance

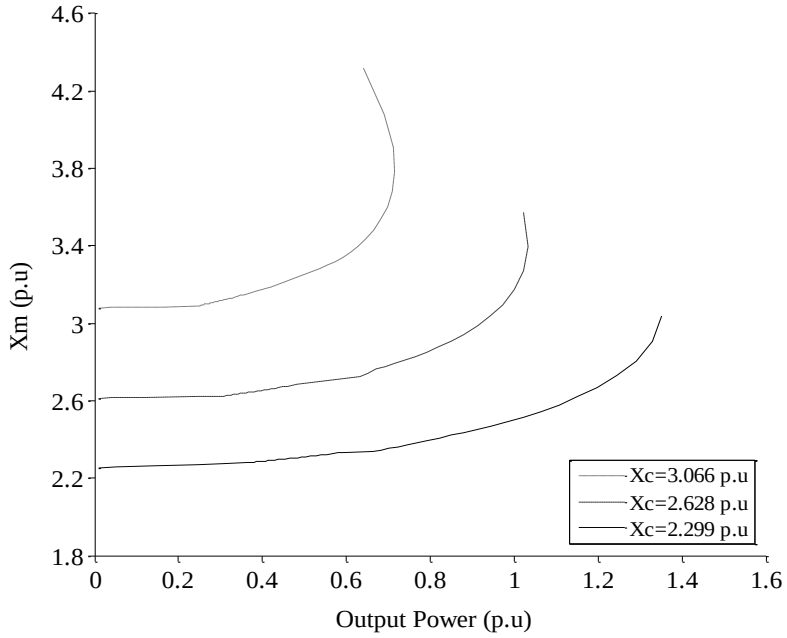

Fig. 2.12 (b): Magnetising reactance v/s Output power

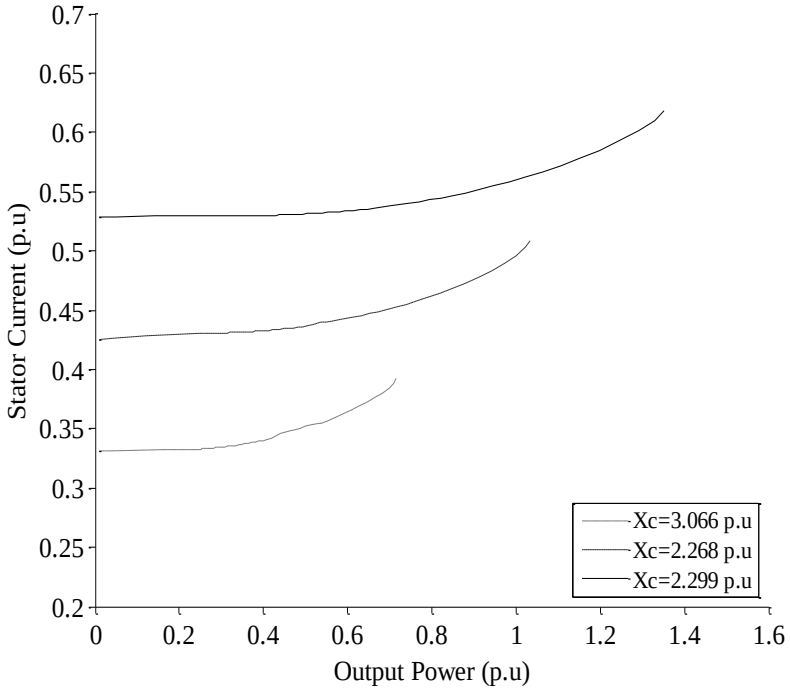

Fig. 2.12 (c): Stator current v/s Output Power

Fig. 2.12 (a) shows the variation of terminal voltage (V_t) with output power (P_{out}). The terminal voltage drops with load. At higher values of C (lower value of X_c) maximum output power is more than the lower value of C (higher value of X_c). The drop in voltage from no-load to full load is considerably less and the initial terminal

voltage is also more for higher value of capacitance, it increases from 1.0 p.u to 1.2 p.u for increase in capacitance from 32.5 μF to 43.5 μF.

Fig. 2.12 (b) shows the variation of magnetizing reactance (X_m) with respect to output power for different values of capacitane, As the loading increases the change in magnetising reactance (X_m) is more prominent for lower values of capacitance (higher value of X_c) than for higher value of capacitance (lower value of X_c) which results in lesser value of terminal voltage (Fig. 2.12 (a))

Fig. 2.12 (c) shows the variation of stator current (I_s) with output power for different values of capacitance. The value of stator current (I_s) is more for higher value of capacitance, which make the machine to handle more loading.

To validate the proposed method, the simulated results are compared with the experimentally measured values on a laboratory machine (specifications given above, machine 2).

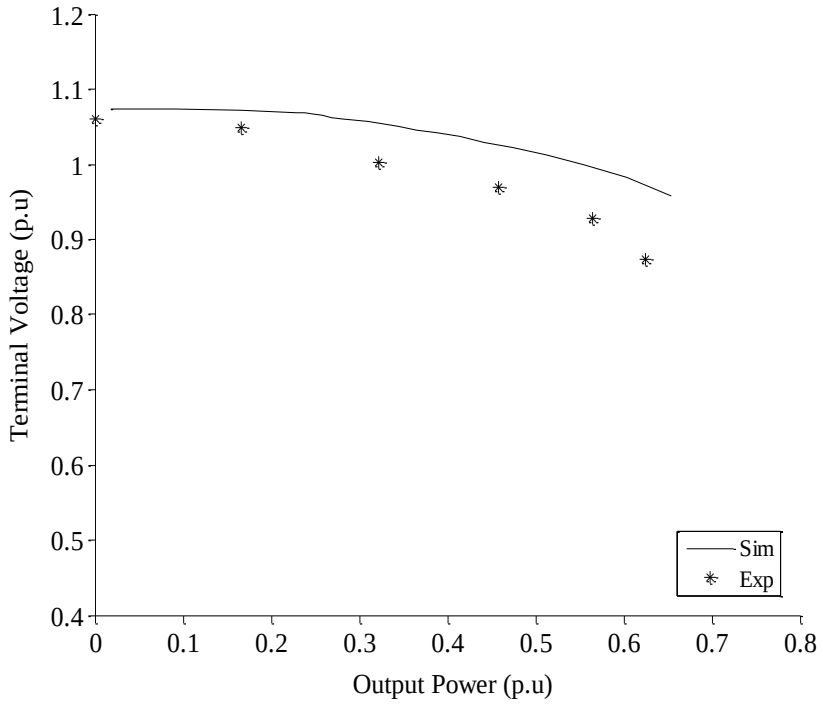

Fig. 2.13.: Terminal Voltage v/s Output Power at 22 µF

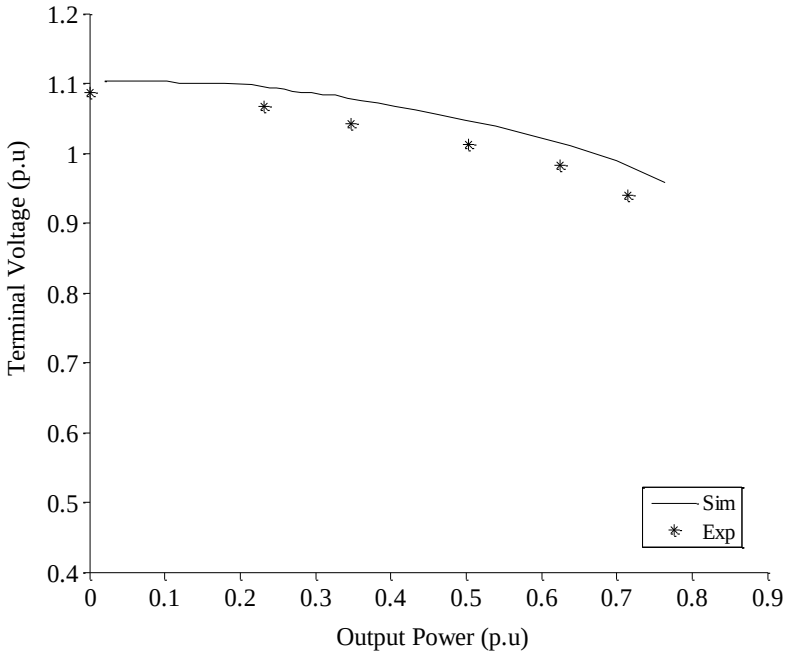

Fig. 2.14: Terminal Voltage v/s Output Power at 24 μF

The Fig. 2.13 and Fig, 2.14 shows simulated and experimental results for terminal voltage v/s output power for the shunt capacitance value, C=22 μF and 24 μF for resistive load with higher capacitance, the output power is increased and results into higher terminal voltage. The output power increased from 0.65 p.u to 0.75 p.u, initial terminal voltage increases from 1.06 p.u to 1.1 p.u. for the change in capacitance from 22 μF to 24 μF.

2.3.3 EFFECT OF VARIATION IN SPEED

Speed of prime mover play an important role in performance of induction generator, speed of prime mover affects the slip of induction generator which further affects the output frequency and terminal voltage. The SEIG performance for speeds as 0.95, 1.0 and 1.05 p.u are shown in Fig. 2.15 for fixed capacitance of 38 μF (X_c=2.628 p.u) for machine 1.

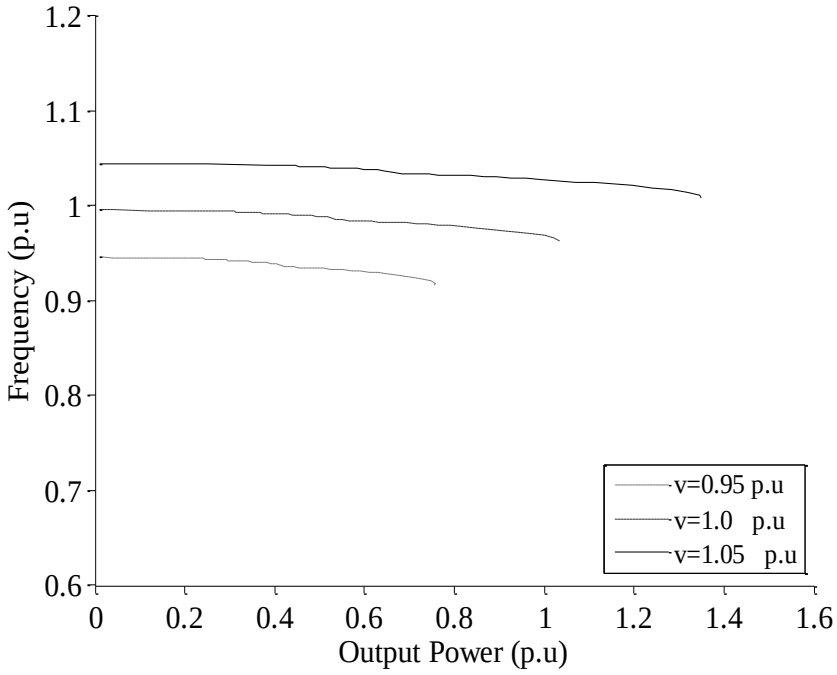

Fig. 2.15 (a): Frequency v/s output power at 38µF for different speeds

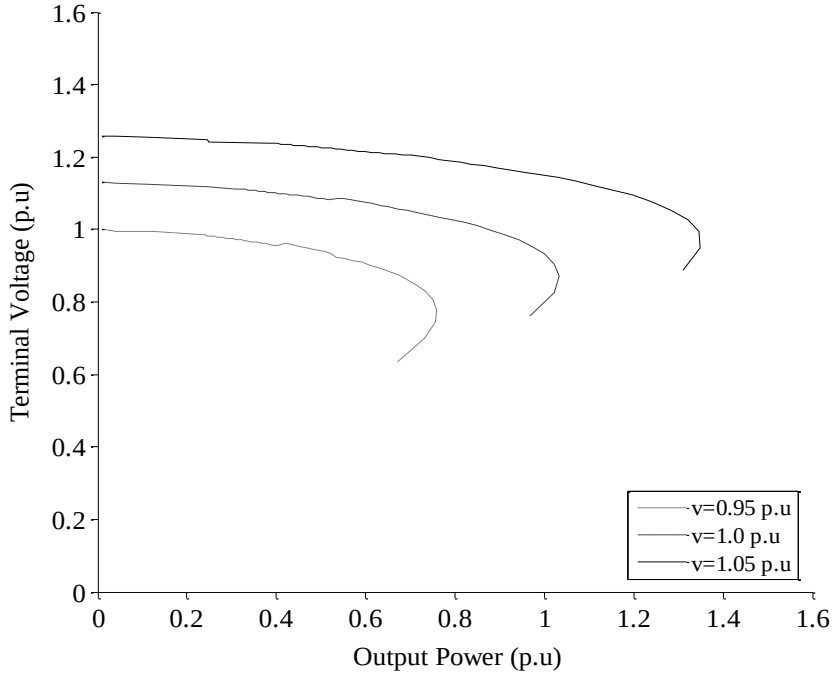

Fig. 2.15 (b): Terminal voltage v/s output Power at 38µF for different speeds

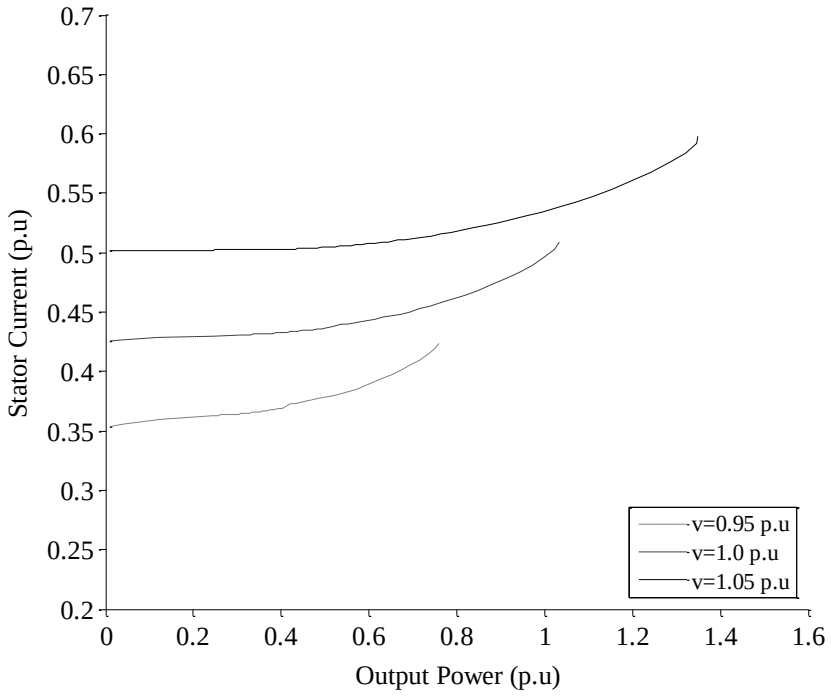

Fig. 2.15 (c): Stator current v/s output power at 38μF for different speeds

Fig. 2.15 (a) shows the variation of output frequency with output power. It is clear that the speed of the prime mover increases the frequency increases. In Fig. 2.15 (a) for an increase in speed form 1.0 p.u to 1.05 p.u the no load frequency increases from 0.99 p.u to 1.04 p.u.

Fig. 2.15 (b) shows the variations of terminal voltage with respect to output power for different values of speeds. The terminal voltage decreases if speed decrease, it changes from 1.25 p.u to 1.0 p.u when speed changes from 1.05 p.u to 0.95 pu. The characteristic also shows that output loading also affected due to changes in speed, output power decreases from 1.4 p.u to 0.8 p.u when speed changes from 1.05 pu to 0.95 pu. For higher values of speed the loading capability of the machine increases.

The change in speed also affects the stator current (I_s) as shown in figure 2.15(c), the value stator current is more for higher value of speed and is less for lesser value of speed. The initial value of current increase from 0.35 pu to 0.5 pu when speed increases from 1.05 pu to 0.95 p.u.

2.4 CONCLUSION

In this chapter the steady state analysis of u SEIG is carried out using fuzzy logic. A computer algorithm of the proposed method has been developed to identify the values of saturated magnetising reactance and the output frequency for given capacitance, speed and load. The performance characteristics are obtained for different values of shunt capacitance and speed change for resistive loading. Terminal voltage depends and loading capability of the machine shunt capacitance. Speed variation also affects the voltage profile and loading capacity. The voltage and loading capacity increase with increase in capacitance and prime-mover speed Simulated results on a laboratory machine are validated experimentally.

CHAPTER 3

ANALYSIS OF SERIES COMPENSATED SEIG USING FUZZY LOGIC

3.1 INTRODUCTION

The steady state analysis of self excited induction generator with simple shunt capacitance has been presented; an obvious disadvantage of the SEIG observed from performance characteristics (Fig. 2.12) is its poor voltage profile. For a given excitation capacitance, the terminal voltage decreases rapidly with increase in loading. When the load impedance is decreased beyond a certain critical value, the machine will enter the unstable operating region, with possible consequence of a complete collapse [26]. Increasing the excitation capacitance causes the machine to operate at a higher saturation level and hence improves the voltage profile, but the increase in magnetizing current and no-load losses may impose a limit on the capacitance that can be used.

Thus researchers have tried various voltage and frequency control schemes in order to improve the voltage stability [64-68]. Many of these control schemes are microprocessor based, which considerably increase the overall cost of the generating plant. For frequency insensitive loads, a simple method to improve the voltage profile without incurring expensive equipment is to use series capacitance compensation. When the load current increases, the current passing through the series capacitance also increases. More magnetising reactive power is provided to the machine, hence the voltage drop with load will be less severe compared with the uncompensated SEIG [30].

Hence, the steady state analysis of SEIG with series capacitance compensation is presented in this chapter. Two different configurations, namely Short-shunt configuration and Long-shunt configuration have been described.

3.2 STEADY STATE ANALYSIS OF SHORT-SHUNT CONFIGURATION

In the self excited induction generator with short-shunt configuration, the compensation capacitance is in series with the load and the shunt capacitance is connected near to the stator terminal of the machine.

C_{sh} is compensation capacitance connected in series,

C is the shunt capacitance.

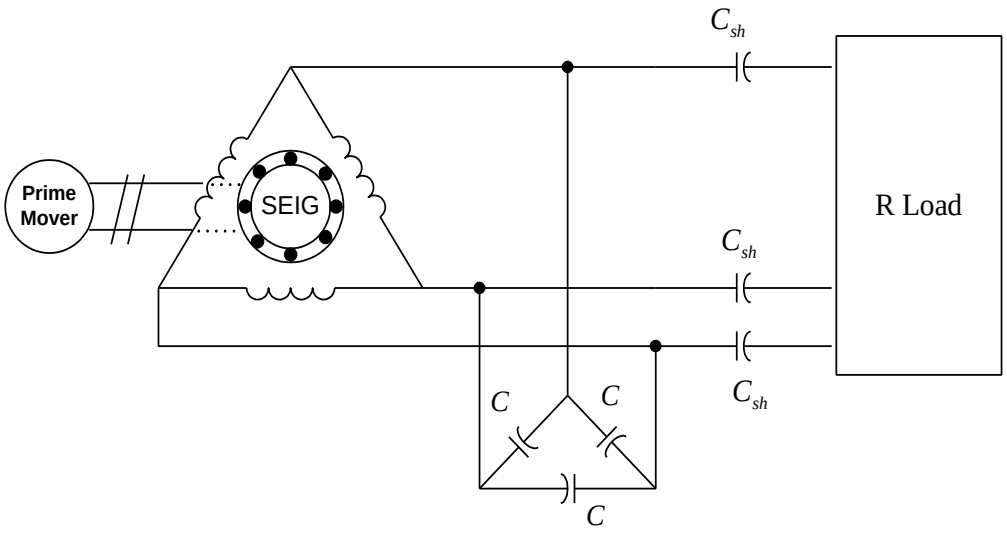

Fig. 3.1: SEIG with Short-Shunt Compensation

The schematic diagram of SEIG with short-shunt configuration is as shown in Fig. 3.1.

The steady state equivalent circuit of a capacitor self excited induction generator with short-shunt compensation for a resistance (R) load connected at terminals is shown in Fig. 3.2.

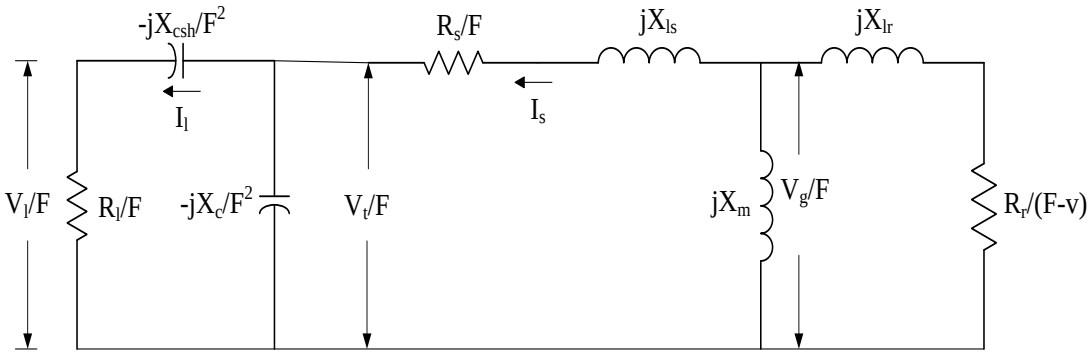

Fig. 3.2: Equivalent circuit of the Short-shunt SEIG

where:

R_s, R_r = per phase stator and rotor (referred to stator) resistance

R_l = per phase load resistance

X_{ls}, X_{lr} = per phase stator and rotor (referred to stator) leakage reactance

X_m = magnetising reactance

X_c = per phase capacitive reactance of the terminal capacitor *C*

X_l = load resistance per phase

X_{csh} = per phase capacitive reactance of the series capacitor C_{sh}

(all reactances referred to above relate to the base frequency F)

F, ϑ = p.u. frequency and speed

I_s, I_r = per phase stator and rotor (referred to stator) current

I_l = per phase load current

$V_t(V_s)$ = terminal or stator voltage

V_g = air gap voltage

V_l = per phase load voltage, respectively.

The various elements of equivalent circuit can be represented as given below.

$$Z_M = jX_m; \qquad Z_{RR} = {R_r}/{(F - \vartheta)} + jX_{lr};$$

$$Z_S = {R_s}/{F} + jR_{ls}; \qquad Z_C = {-jX_c}/{F^2}$$

$$Z_L = {R_l}/{F} - {jX_{csh}}/{F^2}; \qquad X_c = {1}/{\omega C} \text{ and } X_{csh} = {3}/{\omega C_{sh}}$$

From the equivalent circuit of SEIG with short-shunt compensation (Fig. 3.2) and by graph theory approach using loop impedance method the equilibrium equation essential for obtaining the performance characteristics of SEIG is given as,

$$[Z]\,[I] = [0]$$

Where $[Z]$ is the loop impedance matrix,

$$[Z] = \begin{bmatrix} Z_M + Z_{RR} & 0 & Z_{RR} \\ 0 & Z_C + Z_L & Z_L \\ Z_{RR} & Z_L & Z_{RR} + Z_L + Z_S \end{bmatrix}$$

The steady state performance analysis of SEIG with short-shunt compensation is carried out by solving determinant of the loop impedance matrix (det $[Z]$) using fuzzy logic algorithm described below for the unknown quantities, magnetising reactance (X_m) and frequency (F). The fuzzy logic process incorporated in the algorithm (3.2.1) gives incremental values of X_m, is ΔX_m and F, is ΔF.

3.2.1 ALGORITHM FOR FUZZY LOGIC

The Fuzzy Logic Process based computational algorithm for solution of X_m, F and steady state performance of Short-shunt SEIG is as follows:

Step 1: Read all required parameters for matrix$[Z]$.

Step 2: Assume initial values, $X_m = X_{mo}$ and F less than ϑ (p. u. speed) to avoid $R_r/(F-\vartheta) = \infty$, since always $F < \vartheta$.

Step 3: Calculate the real and imaginary part values of the det $[Z]$. Set iteration count, itr =1.

Step 4: Check whether real and imaginary part values of det $[Z]$ reach desired value of tolerance ε, if yes go to step 8 otherwise go to step 5.

Step 5: The real part value of det $[Z]$ is introduced to the 'fuzzy logic process' as explained earlier in section 2.2.3, which results in the incremental change in frequency ΔF.

Step 6: The imaginary part value of det $[Z]$ is introduced to the 'fuzzy logic process' as explained earlier in section 2.2.3, which results in the incremental change in magnetising reactance ΔX_m.

Step 7: Update the values of frequency (F) and magnetising reactance (X_m) as

$F = F + \Delta F$ and $X_m = X_m + \Delta X_m$, Increment the iteration count itr = itr +1 and go to step 3.

Step 8: Compute the performance parameters of the machine and print the results.

Thus, a computer programme has been developed by using the fuzzy logic algorithm to obtain the performance characteristics for SEIG with series compensation.

3.3 PERFORMANCE OF SHORT SHUNT SEIG

The performance characteristics are simulated on the machine 1 having ratings as 4-pole, 50Hz delta connected stator winding rated 230V, 12.5A and 5hp and the specifications are given in Appendix.

3.3.1 PERFORMANCE FOR A GIVEN SHUNT AND SERIES CAPACITANCE

Fig 3.3 shows the typical characteristics of SEIG with Short-shunt compensation feeding resistive load. The above characteristics are plotted for shunt capacitance value of C=38μF (X_c=2.628μF) and a series capacitance value C_{sh}=200μF (X_{csh}=0.4993μF) for constant speed, 1.0 p.u.

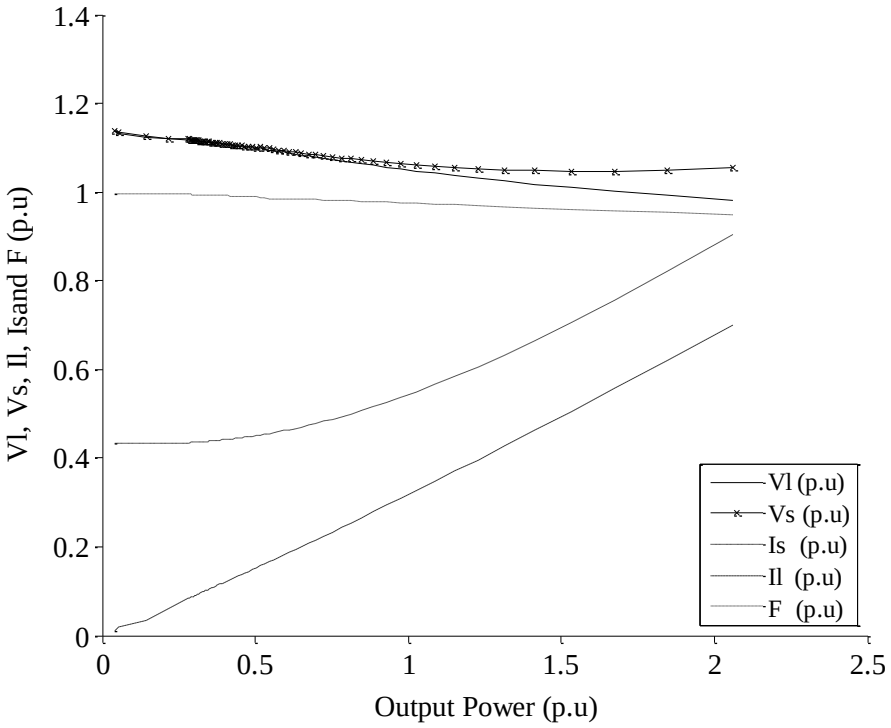

Fig. 3.3: Typical Characteristics of Short-shunt SEIG

From the above characteristics it has been observed that the variation of load voltage with output power is marginal and with inclusion of series capacitance (C_{sh}) results in higher overload capability. Thus, the load voltage (V_l) profile is improved and also the values of stator current (I_s) and load current (I_l) are increased with series capacitance (C_{sh}) compared with the characteristics of SEIG (Fig. 2.10).

3.3.2 EFFECT OF VARIATION OF SERIES CAPACITANCE

The following characteristics are simulated for a fixed value of shunt capacitance (C) and different values of series capacitance (C_{sh}) at a constant speed.

Figs. 3.4(a) to 3.4(d) show the characteristics of short-shunt connections for a fixed value shunt capacitance, C =38 μF (X_c =2.628 p.u) and different values of series capacitance, C_{sh}=180 μF (X_{csh} =0.5548 p.u), C_{sh}=200 μF (X_{csh} =0.4993 p.u), C_{sh}=220 μF (X_{csh} =0.4539 p.u).

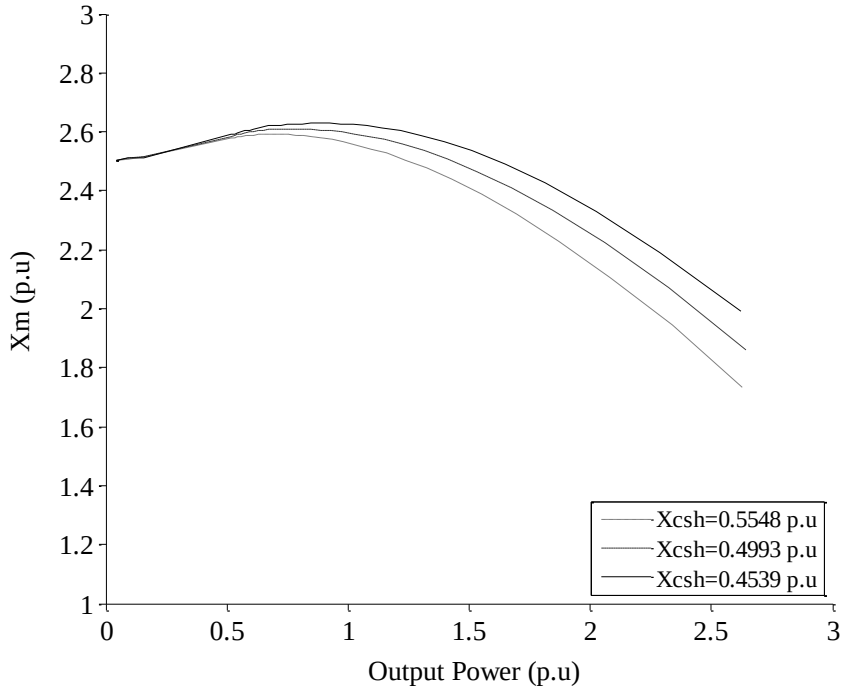

Fig. 3.4 (a): Magnetising reactance v/s output power

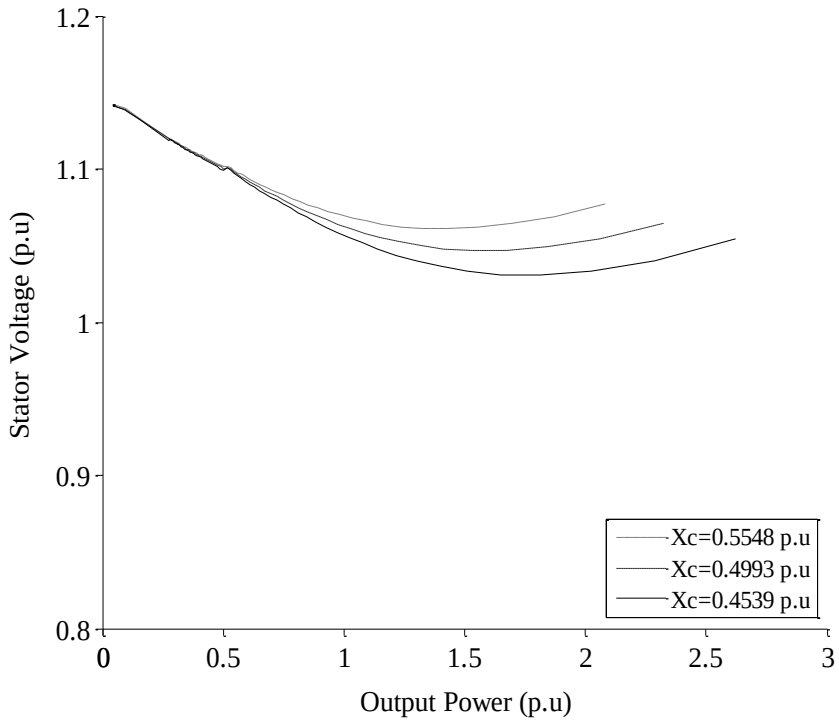

Fig. 3.4 (b): Stator voltage v/s output power

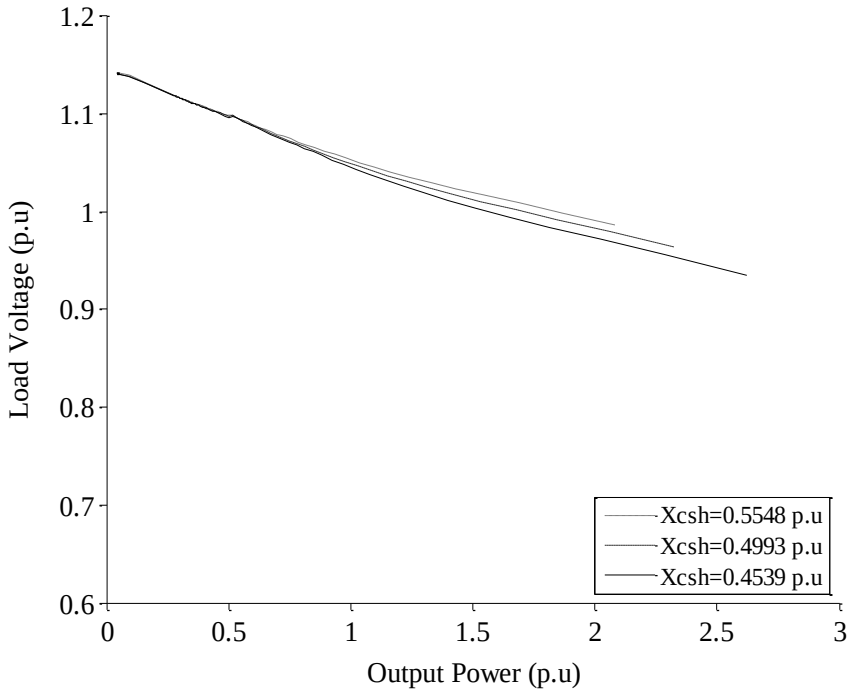

Fig. 3.4 (c): Load voltage v/s output power

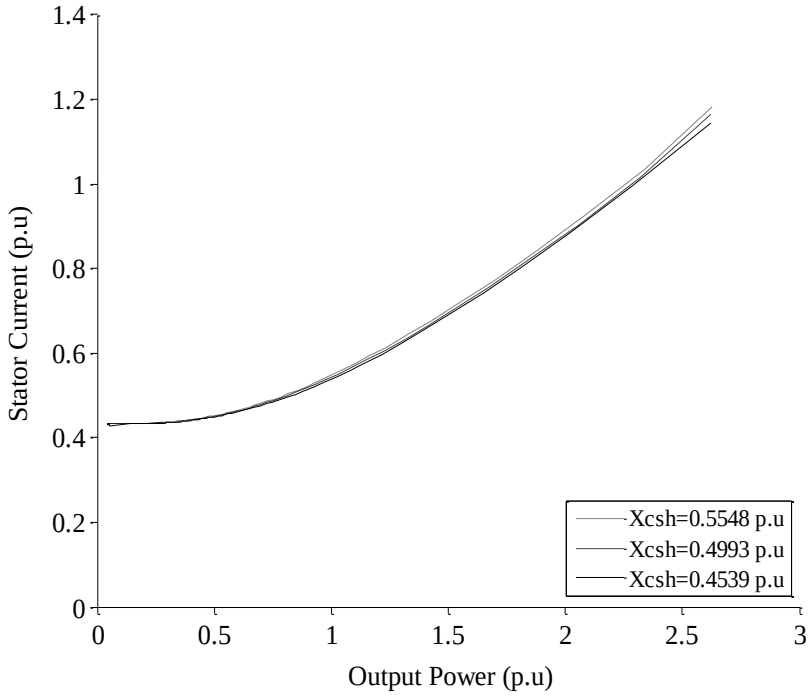

. **Fig. 3.4 (d): Stator current v/s output power**

Fig. 3.4(a) shows the magnetizing reactance versus output real power for short shunt connections. At higher values of output power the magnetising reactance is more for larger value of series capacitance.

Fig. 3.4(b) shows the stator voltage (V_s) versus output power for short-shunt connections. The stator voltage (V_s) decreases under lower output powers and increases under higher output powers. Since the magnetizing reactance greatly affects the stator voltages of induction generator, under higher output powers, the magnetizing reactance value decreases (Fig. 3.4(a)), hence the corresponding terminal voltage increases (Fig. 3.4(b)). It is also observed that the lower the series capacitance values, the terminal voltages are higher. At a loading of 2.0 p.u, for a change in series capacitance C_{sh}=180 μF (X_{csh} =0.5548 p.u), to C_{sh}=220 μF (X_{csh} =0.4539 p.u) the stator voltage (V_s) decreases from 1.05 p.u to 1.01 p.u (Fig. 3.4(b)).

Fig. 3.4(c) shows the load voltage (V_l) versus output real power for short-shunt connections. It is observed that the voltage variations are less from no load to rated

load conditions. It is also observed that under higher output powers, the lower the series capacitance values, the terminal voltages are higher.

Fig. 3.4(d) shows the characteristics of stator current versus output real power for short-shunt connections. The stator winding current are well below the rated value at rated output real power. It has been observed that the characteristics of stator currents v/s output power overlaps for different values of series capacitance (C_{sh}).

3.3.3 EFFECT OF VARIATION OF SHUNT CAPACITANCE

The following characteristics of given machine with short shunt compensation are observed for a fixed value of series capacitance (C_{sh}) and different values of shunt capacitance (C).

Figs. 3.5(a) and 3.5(b) show the characteristics of short-shunt connections for a fixed value series capacitance C_{sh}=200 μF (X_{csh} =0.4993 p.u), and different values of shunt capacitance, C=32.5 μF (X_c =3.066 p.u); C=38 μF (X_c =2.628 p.u) and C=43.5 μF (X_c =2.299 p.u).

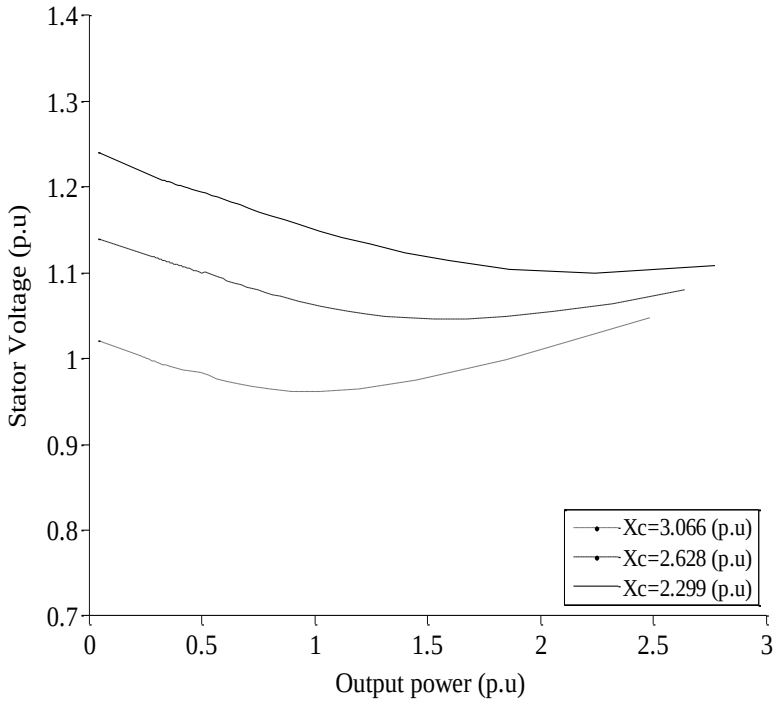

Fig.3.5 (a) Stator voltage v/s output power at C_{sh}= 200μF

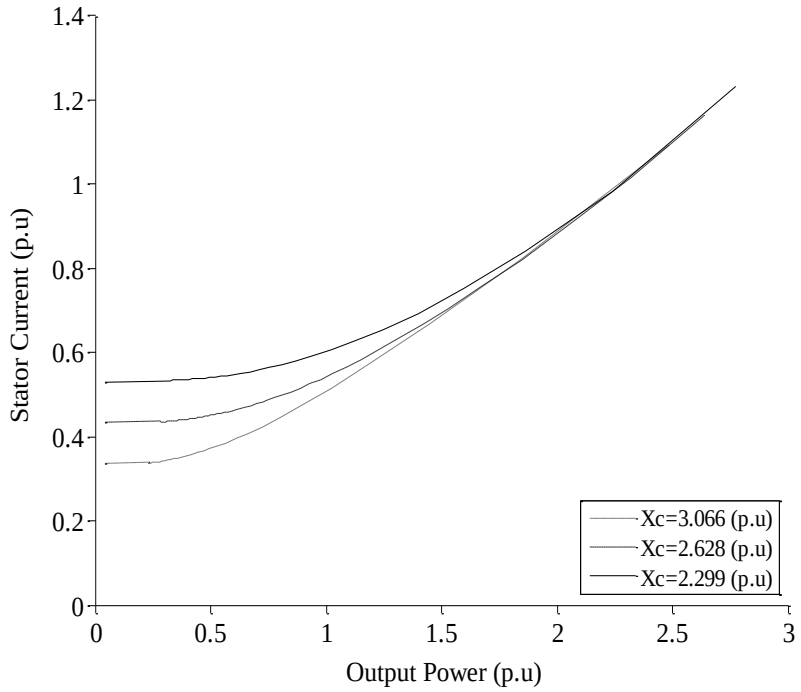

Fig.3.5 (b) Stator current v/s output power at C_{sh}= 200μF

In Figs. 3.5 (a) the stator voltage is high for higher values of capacitance and it is also observed that for higher values of capacitance the capability of the machine increases i.e. the machine is able to deliver more than rated power output the stator voltage increases from 1.01 pu to 1.23 p.u for a increase in shunt capacitance from 32.5 μF to 43.5 μF.

Fig .3.5 (b) shows the variation stator current for higher output is less, even when the shunt capacitance value changes. For the no-load condition stator currents are more for higher values of shunt capacitance.

3.3.4 EFFECT OF VARIATION IN SPEED

The following characteristics of given machine with short shunt compensation are observed for a different values speed change with a fixed series capacitance (C_{sh}) and shunt capacitance (C).

Fig.3.6. (a) to Fig. 3.6 (b) shows the various performance characteristics for different values of speed ϑ =0.95p.u, ϑ =1.0 p.u and ϑ=1.05 at fixed shunt capacitance C=38 μF, X_c=2.628 and series capacitance C_{sh}=200 μF (X_{csh} =0.4993 p.u).

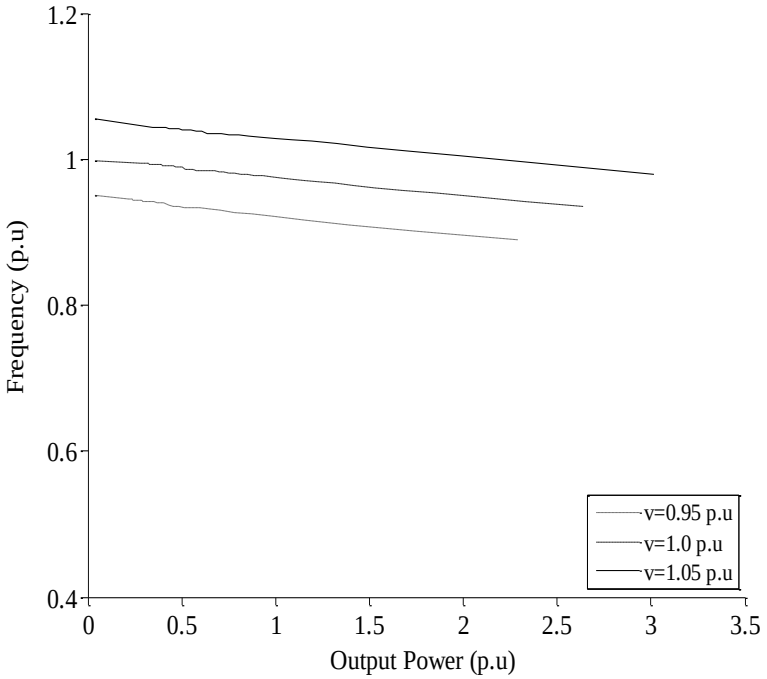

Fig. 3.6 (a): Frequency v/s output power for different speeds

Fig. 3.6 (a) shows the variation of output frequency with output power for different values of speed, it is clear that the speed of the prime mover increases the frequency increases. In Fig. 3.6 (a) for an increase in speed from 1.0 p.u to 1.05 p.u the no load frequency increases from 0.95 p.u to 1.03 p.u.

Fig. 3.6 (b) shows the stator voltage versus output power for different values of speeds. The variation of stator voltage is more at low power output, it changes from 1.29 pu to 1.01 pu for a speed change from 1.05 pu to 0.95 pu. The characteristic also shows that output power also affected due to changes in speed, output power decreases from 2.8 pu to 2.3 pu when speed changes from 1.05 pu to 0.95 pu. For higher values of speed the loading capability of the machine increases.

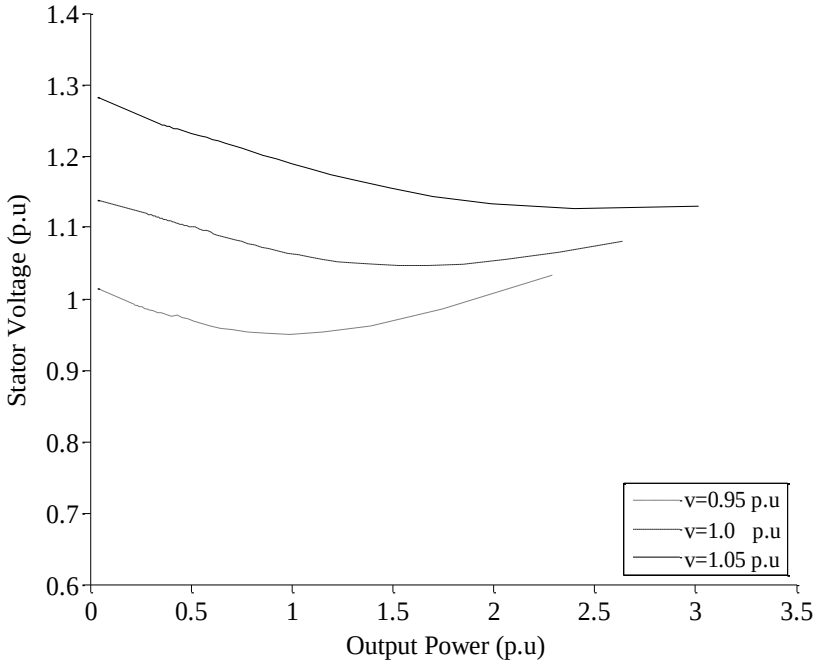

Fig. 3.6 (b): Stator voltage v/s output power for different speeds

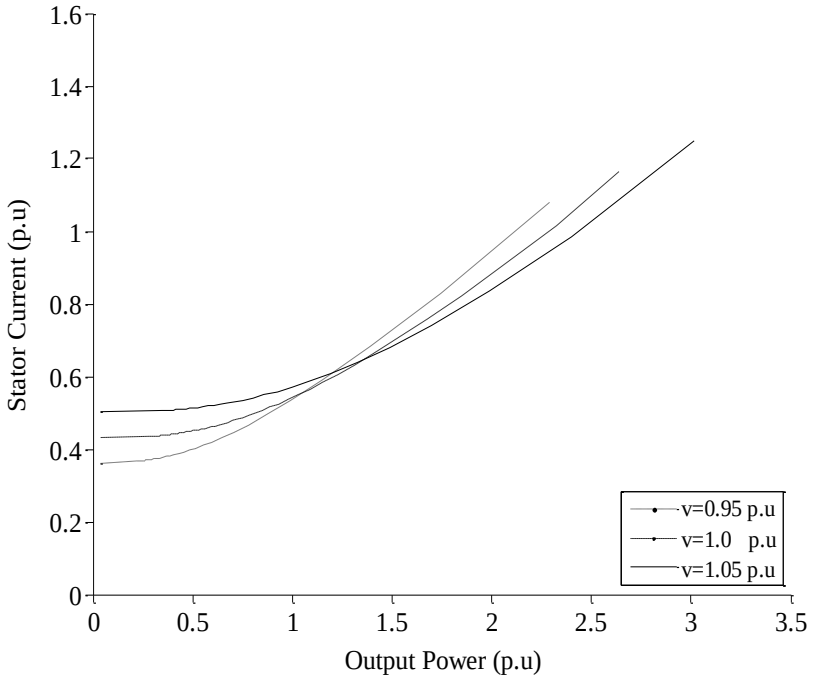

Fig. 3.6 (c): Stator current v/s output power for different speed

The change in speed affects the stator current (I_s) as shown in figure 2.17, the value stator current is more for higher value of speed and is less for lesser value of speed. The initial value of current increase from 0.35 pu to 0.5 pu when speed increases from 1.05 pu to 0.95 pu.

3.4 STEADY STATE PERFORMANCE OF LONG-SHUNT CONFIGURATION

In the self excited induction generator with long-shunt configuration, the compensation capacitance is in series with the stator terminals of the machine and the shunt capacitance is connected near to the load.

C_{lo} is compensation capacitance connected in series,

C is the shunt capacitance.

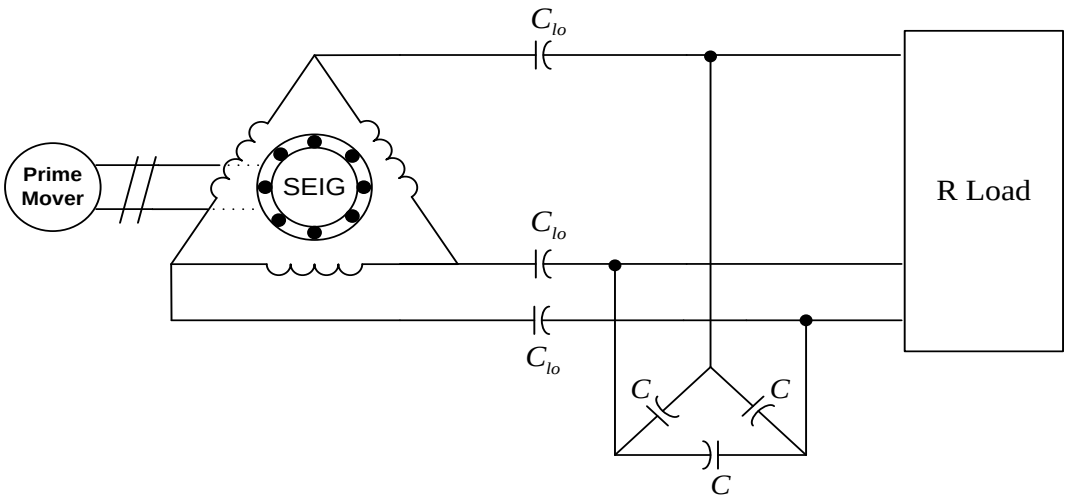

Fig. 3.7: SEIG with Long-Shunt Compensation

The schematic diagram of SEIG with long-shunt configuration is as shown in Fig. 3.7, where

The steady state equivalent circuit of a capacitor self excited induction generator with long-shunt compensation for a resistive (R) load connected at terminals is shown in Fig. 3.8.

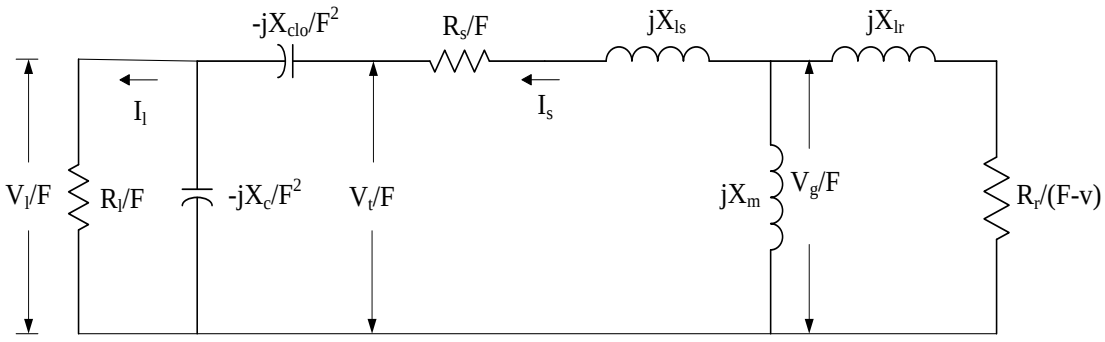

Fig. 3.8: Equivalent circuit of the Long-shunt SEIG

where:

R_s, R_r = per phase stator and rotor (referred to stator) resistance

R_l = per phase load resistance

X_{ls}, X_{lr} = per phase stator and rotor (referred to stator) leakage reactance

X_m = magnetising reactance

X_c = per phase capacitive reactance of the terminal capacitor *C*

X_l = load resistance per phase

X_{clo} = per phase capacitive reactance of the series capacitor C_{lo}

(all reactances referred to above relate to the base frequency F)

F, ϑ = p.u. frequency and speed

I_s, I_r = per phase stator and rotor (referred to stator) current

I_l = per phase load current

$V_t(V_s)$ = terminal or stator voltage

V_g = air gap voltage

V_l = per phase load voltage, respectively.

The various elements of equivalent circuit can be represented as given below.

$$Z_M = jX_m; \qquad Z_{RR} = {R_r}/{(F - \vartheta)} + jX_{lr};$$

$$Z_S = {R_s}/{F} + jX_{ls} - {jX_{clo}}/{F^2}; \qquad Z_C = {-jX_c}/{F^2}$$

$$Z_L = {R_l}/{F}; \qquad \text{and} \qquad X_{clo} = {3}/{\omega C_{lo}}$$

From the equivalent circuit of SEIG with long-shunt compensation (Fig. 3.6) and by graph theory approach using loop impedance method the equilibrium equation essential for obtaining the performance characteristics of long-shunt SEIG is given as,

$$[Z]\,[I] = [0]$$

where $[Z]$ is the loop impedance matrix,

$$[Z] = \begin{bmatrix} Z_M + Z_{RR} & 0 & Z_{RR} \\ 0 & Z_C + Z_L & Z_L \\ Z_{RR} & Z_L & Z_{RR} + Z_L + Z_S \end{bmatrix}$$

The steady state performance analysis of SEIG with long-shunt compensation is carried out by solving determinant of the loop impedance matrix (det $[Z]$) using fuzzy logic algorithm discussed earlier for the unknown quantities, magnetising reactance (X_m) and frequency (F).

A computer programme has been developed by using the proposed fuzzy logic algorithm as discussed in section 3.2.1.

3.5 PERFORMANCE OF LONG SHUNT SEIG

The performance characteristics are simulated on the machine 1 having ratings as 4-pole, 50Hz delta connected stator winding rated 230V, 12.5A and 5hp and the specifications are given in Appendix.

3.5.1 PERFORMANCE FOR A GIVEN SHUNT AND SERIES CAPACITANCE

The performance characteristics have been plotted for the above given machine for a fixed value of shunt capacitance (C) and a series capacitance (C_{lo}) at constant speed (ϑ=1.0 p.u)

Fig. 3.9 shows the typical characteristics of SEIG with Long-shunt compensation feeding resistive load. The above characteristics are plotted for shunt capacitance value of C=43.5μF and a series capacitance value C_{lo}=270μF.

From the above characteristics it has been observed that the variation of load voltage with output power is marginal and with inclusion of series capacitance (C_{lo}) results in higher overload capability. Thus, the load voltage (V_l) profile is improved and also the values of stator current (I_s) and load current (I_s) are increased with series capacitance. Due to the voltage drop across the series capacitance, the load voltage (V_l) is lower than the machine stator voltage (V_s).

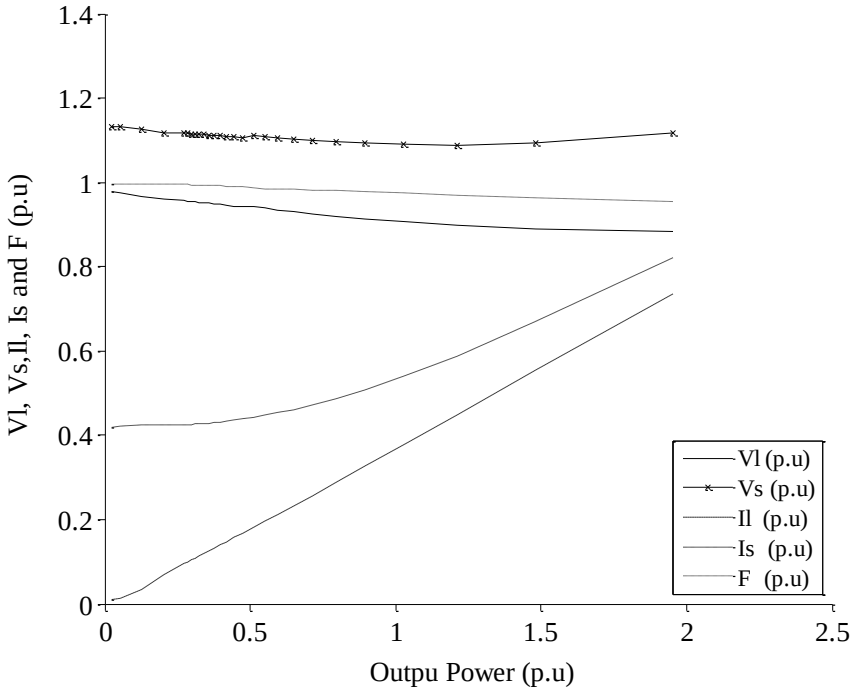

Fig. 3.9: Load Characteristics of Long-shunt SEIG

3.5.2 EFFECT OF VARIATION OF SERIES CAPACITANCE

The following characteristics are simulated for a fixed value of shunt capacitance (C) and different values of series capacitance (C_{lo}) at a constant speed.

The characteristics of long-shunt connection shown in Fig. 3.10 (a) – Fig. 3.10 (d) are obtained for a fixed value of excitation capacitance C =43.5 μF (X_c =2.299 p.u) .Three series capacitance values, C_{lo}=240 μF (X_{clo} =0.4161 p.u) C_{lo}=270 μF (X_{clo} =0.3699 p.u), C_{lo}=300 μF (X_{clo} =0.3329 p.u) for long-shunt connections were employed to study the performance of the long-shunt SEIG.

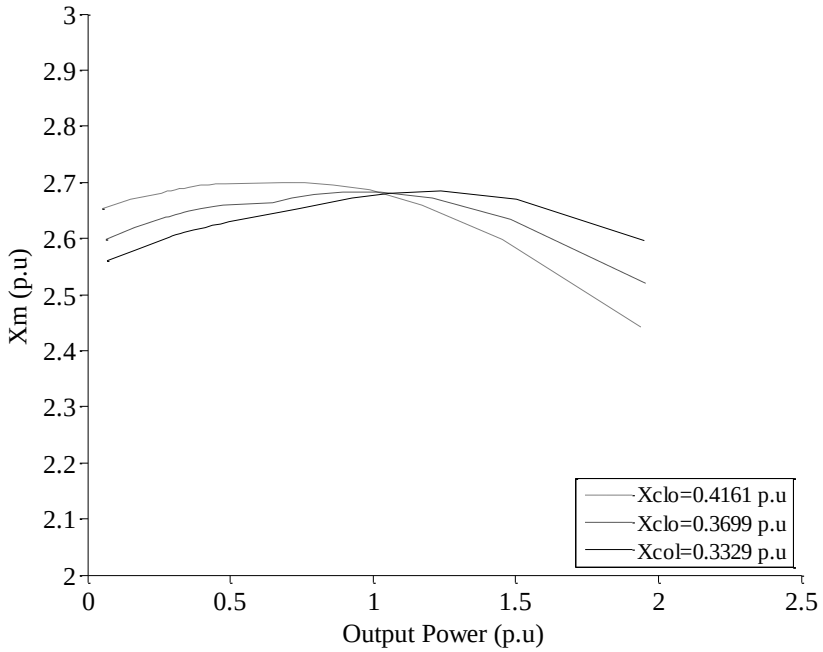

Fig. 3.10 (a): Magnetising reactance v/s output power

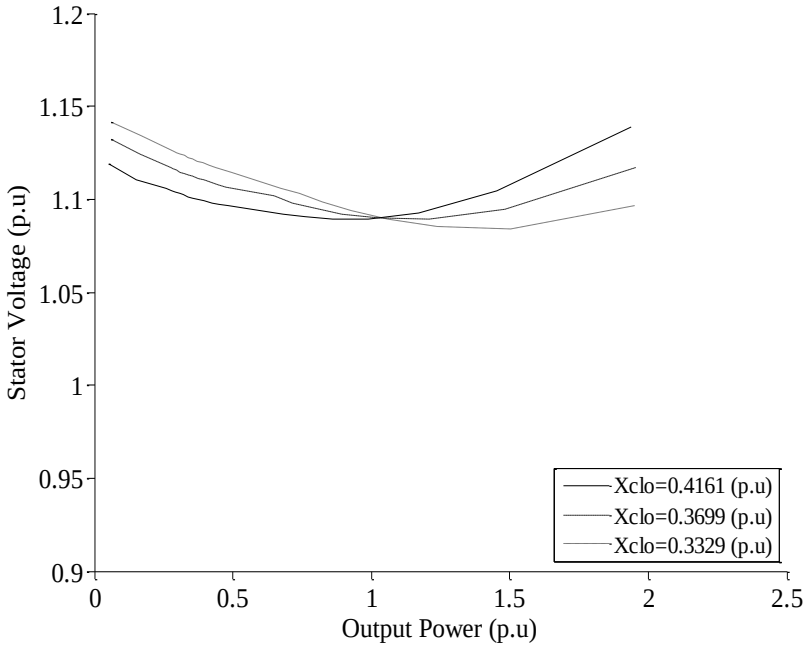

Fig. 3.10 (b): Stator voltage v/s output power

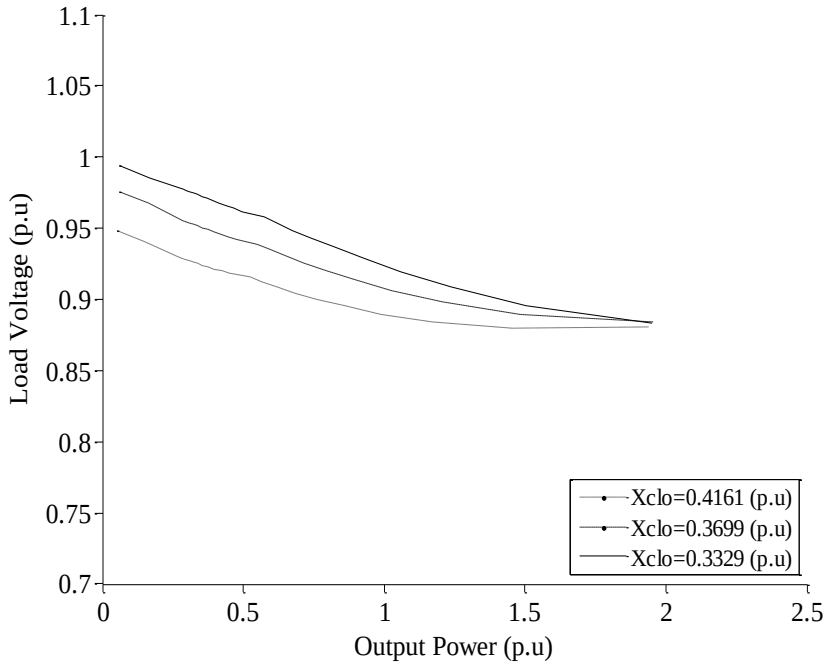

Fig. 3.10 (c): Load voltage v/s output power

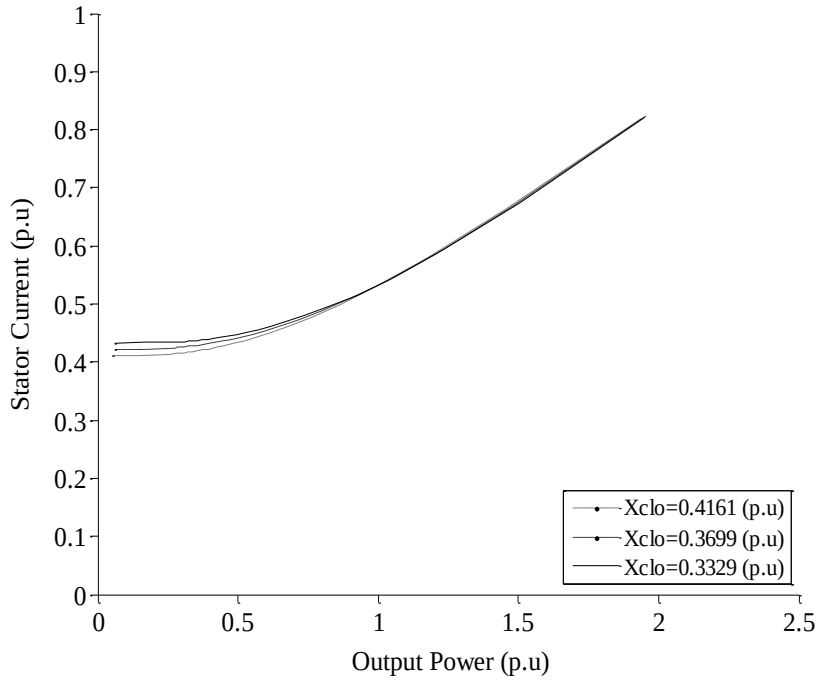

Fig. 3.10 (d): Stator current v/s output power

Fig. 3.10 (a) shows the magnetizing reactance versus output real power for long-shunt connections. At higher values of output power the magnetising reactance is more for larger value of series capacitance (C_{lo}=300μF) and at lower values of power

output, X_m is high for lower values of series capacitance (C_{lo}=240μF). From Fig.3.8 (a), it is observed that the X_m increases for lesser values of loading and then it decrease for higher values of loading.

Fig. 3.10(b) shows the stator voltage (V_s) versus output power for long-shunt connections. The long-shunt connection has larger voltage variations under higher output powers. The stator voltage (V_s) decreases under lower output powers and increases under higher output powers. Since the magnetizing reactance (X_m) greatly affects the stator voltages of induction generator, Fig. 3.10(b) has opposite variations with respect to Fig. 3.10(a), under higher output powers, the magnetizing reactance value decreases (Fig. 3.10(a)), hence the corresponding stator voltage (V_s) increases (Fig. 3.10(b)). Also under higher output real powers, the lower the series capacitance values, the terminal voltages are higher. At a loading of 2.0 p.u, for a change in series capacitance, C_{lo}=240 μF (X_{clo} =0.4161 p.u) to C_{lo}=300 μF (X_{clo} =0.3329 p.u) the stator voltage decreases from 1.1 p.u to 1.15 p.u (Fig. 3.10(b)).

Fig. 3.10(c) shows the load voltage (V_l) versus output power for long-shunt connections. It is observed that the voltage variations are low for different values of series capacitance at rated load conditions. The load voltages are more for higher values of series capacitance at lower load condition.

Fig. 3.10(d) shows the characteristics of stator current versus output power for short-shunt connections. The stator winding current are well below the rated value at rated output power. It has been observed that the characteristics of stator currents (I_s) versus output power overlaps for different values of series capacitance (C_{lo}).

3.5.3 EFFECT OF VARIATION OF SHUNT CAPACITANCE

The following characteristics of given machine with Long shunt compensation are observed for a fixed value of series capacitance (C_{lo}) and different values of shunt capacitance (C).

Figs. 3.11(a) and 3.11(b) show the characteristics of Long-shunt connections for a fixed value series capacitanceC_{lo}=270 μF (X_{clo} =0.3699 p.u), and different values of shunt capacitance, C=32.5 μF (X_c =3.066 p.u); C=38 μF (X_c =2.628 p.u) and C=43.5 μF (X_c =2.299 p.u).

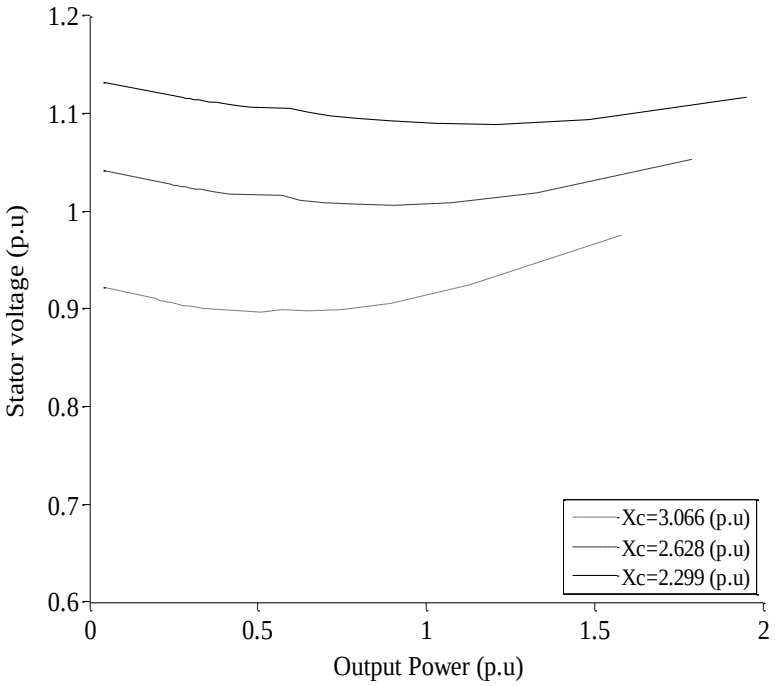

Fig. 3.11 (a): Stator voltage v/s output power at C_{lo}=270 μF

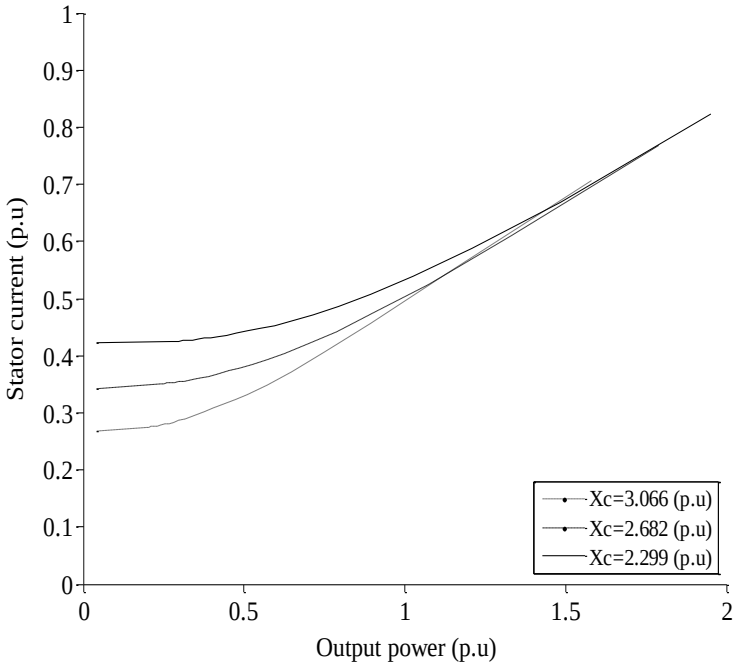

Fig. 3.11(b): Stator current v/s output power at C_{lo}=270 μF

In Figs. 3.11 (a) the stator voltage is high for higher values of capacitance and it is also observed that for higher values of capacitance the capability of the machine

increases i.e. the machine is able to deliver more than rated power output the stator voltage increases from 0.92 pu to 1.14 p.u for a increase in shunt capacitance from 32.5 μF to 43.5 μF.

Fig .3.11 (b) shows the variation stator current for higher output is less, even when the shunt capacitance value changes. For the no-load condition stator currents are more for higher values of shunt capacitance.

3.5.4 EFFECT OF VARIATION IN SPEED

The following characteristics of given machine with Long shunt compensation are observed for a different values speed change with a fixed series capacitance (C_{lo}) and shunt capacitance (C).

Fig.3.12. (a) to Fig. 3.12 (c) shows the various performance characteristics for different values of speed ϑ =0.95p.u, ϑ =1.0 p.u and ϑ=1.05 at fixed shunt capacitance C=38 μF, (X_c=2.628 p.u) and series capacitance C_{lo}=270 μF (X_{csh} =0.3699 p.u).

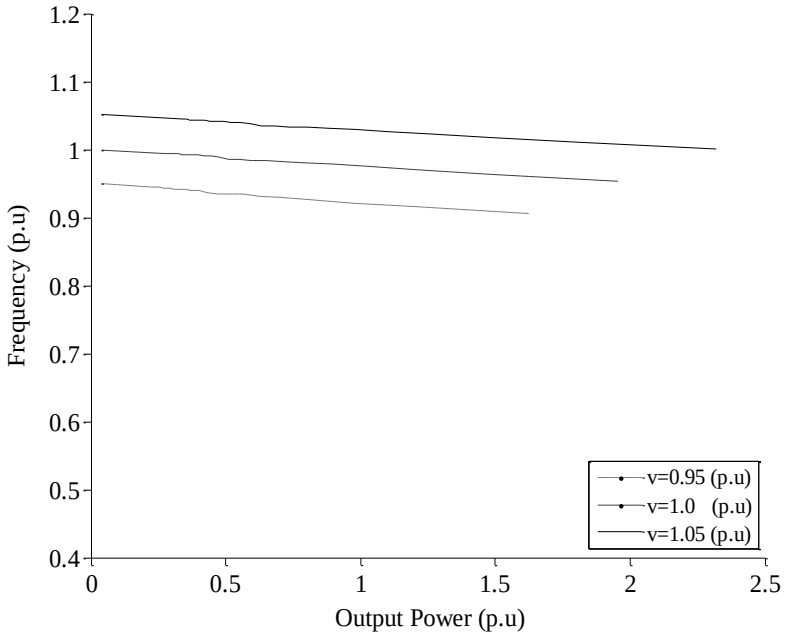

Fig. 3.12 (a): Frequency v/s output power for different speeds

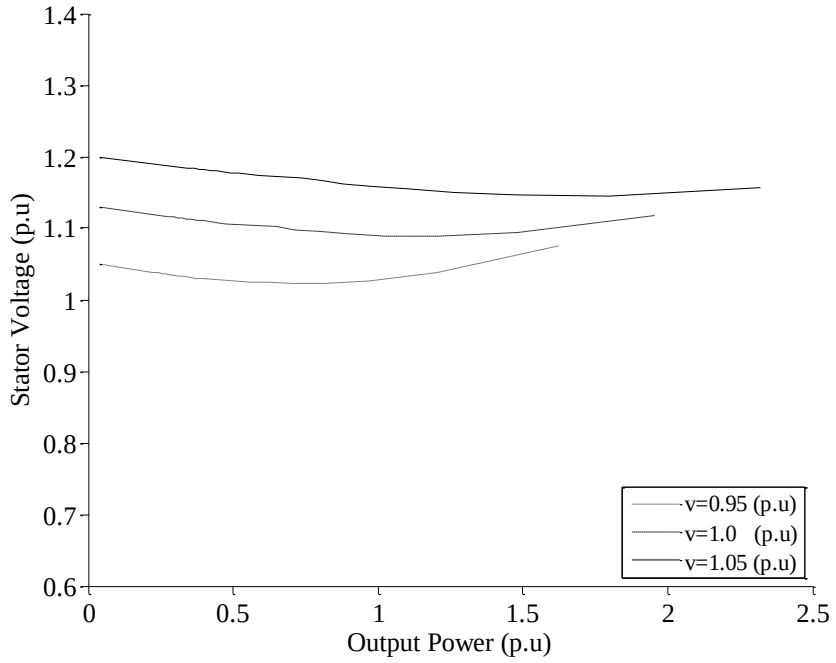

Fig. 3.12 (b): Stator voltage v/s output power for different speeds

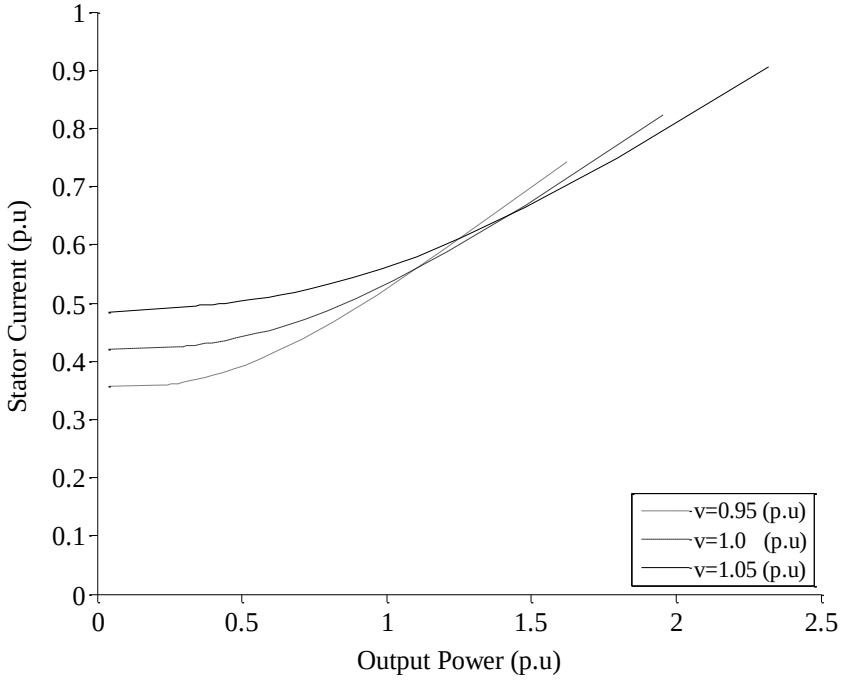

Fig. 3.12 (c): Stator current v/s speed for different speeds

Fig. 3.12 (a) shows the variation of output frequency with output power for different values of speed, it is clear that the speed of the prime mover increases the frequency increases. In Fig. 3.12 (a) for an increase in speed from 1.0 p.u to 1.05 p.u the no load frequency increases from 0.95 p.u to 1.05 p.u.

Fig. 3.12 (b) shows the stator voltage versus output power for different values of speeds. The variation of stator voltage is more at low power output, it changes from 1.2 pu to 1.05 pu for a speed change from 1.05 pu to 0.95 pu. The characteristic also shows that output power also affected due to changes in speed, output power decreases from 2.4 pu to 1.7 pu when speed changes from 1.05 pu to 0.95 pu. For higher values of speed the loading capability of the machine increases.

The change in speed affects the stator current (I_s) as shown in figure 3.12 (c), the value stator current is more for higher value of speed and is less for lesser value of speed. The initial value of current increase from 0.35 pu to 0.48 pu when speed increases from 1.05 pu to 0.95 pu.

3.6 CONCLUSION

In this chapter the steady state analysis of Short-shunt SEIG and Long-shunt SEIG are carried out using fuzzy logic. A computer algorithm of method has been developed to calculate the values of magnetising reactance and the output frequency for given capacitances, speed and load. The steady state equivalent circuit is used to compute the performance. The performance is also simulated to study the effect of shunt capacitance and series capacitance. The short shunt SEIG requires lower values of capacitances compared to respective long shunt capacitances value.

The performance of both the configurations is sensitive to variation in shunt capacitance value compared to variation in series capacitance value. The performance is also studied for varying speed. As expected, the higher voltage and higher loading is resulted at higher speed.

CHAPTER 4

CONCLUSION AND FUTURE SCOPE OF WORK

4.1 CONCLUSIONS

Use of self excited induction generator is becoming popular for the renewable energy sources because of its isolated mode of operation. Steady state analysis of such generator is of interest, both from design and operational point of view. In the present work the steady state analysis of an SEIG with and without series compensation has been carried out using fuzzy logic. A computer algorithm using the proposed method has been developed identifies the values of saturated magnetising reactance and the output frequency for given capacitance, speed and load.

The performance characteristics of a given machine are obtained for different values of shunt capacitance and speed change with resistive loading. Terminal voltage depends upon shunt capacitance value, if the value of shunt capacitance increases the value of terminal voltage increases and loading capability of the machine also increases. Speed variation also affects the voltage of SEIG. The terminal voltage increases if the speed of the prime mover increases, shunt capacitance further improve the performance of SEIG if the speed of prime mover change. Simulated results on a laboratory machine compare favourably with the experimental values.

The steady state performance of series compensated SEIG i.e. short shunt and long shunt SEIG is simulated using fuzzy logic approach for specified capacitances. The effect of capacitances and prime-mover speed is also studied.

It is observed that by using an additional capacitance in series with load, it is possible to obtain almost flat load voltage profile and the SEIG can deliver load in excess of rated value. The higher values of series and shunt capacitances are needed for long shunt SEIG. Further the stator voltage and stator current remains higher than the respective short shunt SEIG values.

4.2 SCOPE FOR FUTURE WORK

(i) The application of fuzzy logic approach can be tested for resistance-reactance (R-L) loads.

(ii) The effectiveness of the method can be tested for obtaining X_c for constant voltage operation etc.

REFERENCES

[1] R. C. Bansal, T. S. Bhatti, and D. P. Kothari, "A bibliographical survey on induction generators for application of nonconventional energy systems," *IEEE Transactions on Energy Conversion*, vol. 18, no. 3, pp. 433–439, Sep. 2003.

[2] R. C. Bansal, "Three phase self excited induction generator: An Overview," *IEEE Transaction on Energy Conversion*, vol. 20, no. 2, pp. 292-299, Jun. 2005.

[3] S. S. Murthy, B. P. Singh, C. Nagamani and K. V. V. Satyanarayana, "Studies on the use of conventional induction motors as self excited induction generators," *IEEE Transactions on Energy Conversion*, vol. 3, no. 4, pp. Dec 1988.

[4] M. G. Simoes and F. A. Farret, "Renewable energy systems: Design and analysis with induction generators," CRC Press, Boca Raton, FL, 2004.

[5] I. Boldea, "Variable speed generators: The electric generator handbook," CRC Press, Boca Raton, FL, 2006.

[6] I. Cadirci and M. Ermis, "Double-output induction generator operating at sub-synchronous and supersynchronous speeds: Steady-state performance optimization and wind-energy recovery," *IEE Proceedings on Electric Power Applications*, vol. 139, pp. 429–442, 1992.

[7] S. Wekhande and V. Agarwal, "A new variable speed constant voltage controller for self-excited induction generator," *Electric Power System Research*, vol. 59, no. 3, pp. 157 - 164, 2001.

[8] T. F. Chan, "Self-excited induction generators driven by regulated and unregulated turbines," *IEEE Transations on Energy Conversion*, vol. 11, pp. 338–343, June 1996.

[9] G. A. Smith and D. M. Donegani, "A variable-speed constant-frequency induction generator for sub and super synchronous operation," in *Proceeding of European Wind Energy Association Conference*, Rome, Italy, 1986.

[10] B. Singh, "Induction generator-A prospective," *Electric Machines and Power Systems*, vol. 23, pp. 163–177, 1995.

[11] P. K. S. Khan and J. K. Chatterjee, "Three-phase induction generators: A discussion on performance," *Electric Machines Power Systems*, vol. 27, pp. 813–832, 1998.

[12] B. C. Doxy, "Theory and application of the capacitor-excited induction generator," *The Engineer*, vol. 216, pp. 893–897, 1963.

[13] J. M. Elder, J. T. Boys and J. L.Woodward, "The process of self excitation in induction generators," *IEE Proceedings on Electric Power Applications*, vol. 130, no. 2, pp. 103–108, Mar. 1983.

[14] E. Levy and Y. W. Liao, "An experimental investigation of self-excitation in capacitor excited induction generators," *Electric Power System Research*, vol. 53, pp. 59–65, 2000.

[15] T. Ahmed, O. Noro, K. Matzuo, Y. Shindo and M. Nakaoka, "Minimum excitation capacitance requirements for wind turbine coupled stand-alone self-excited induction generator with voltage regulation based on SVC," *IEEE Proceeding on Telecommunication Energy*, pp. 396 – 403, Oct. 2003.

[16] L. Wang and J. Y. Su, "Determination of minimum and maximum capacitances of an isolated SEIG using eigen value sensitivity approach," *IEEE Proceedings on Power System Technology*, vol. 1, pp. 610 – 614, Aug. 1998.

[17] R. C. Bansal, T. S. Bhatti and D. P. Kothari, "Some aspects of grid connected wind electric energy conversion systems," *Interdisciplinary J. Inst. Eng. (India)*, vol. 82, pp. 25–28, May 2001.

[18] S. S. Murthy, O. P. Malik and A. K. Tandon, "Analysis of self-excited induction generators,"*IEE Proceeding on*, vol. 129, no. 6, pp. 260–265, Nov. 1982.

[19] L. Quazene and G. McPherson, "Analysis of the isolated induction generator," *IEEE Transactions on Power Apparatus Systems*, vol. 102, pp. 2793–2798, Aug. 1983.

[20] A. K. Tandon, S. S. Murthy and G. J. Berg, "Steady state analysis of capacitor self-excited induction generators," *IEEE Transactions Power Apparatus Systems*, vol. PAS-103, no. 3, pp. 612–618, Mar. 1984.

[21] A. K. Tandon, S. S. Murthy, and C. S. Jha, "New method of computing steady state response of capacitor self-excited induction generators," *J. Inst. Eng. (India) Electr. Eng.*, vol. 65, pp. 196–201, June 1985.

[22] N. H. Malik and S. Haque, "Steady state analysis and performance of an isolated self-excited induction generator," *IEEE Transactions on Energy Conversion*, vol. EC-1, pp. 130–140, Sept. 1986.

[23] A. H. Al-Bahrani and N. H. Malik, "Steady-state analysis and performance characteristics of a three-phase induction generator self-excited with a single capacitor," *IEEE Transactions on Energy Conversion*, vol. 5, pp. 725–732, Dec. 1990.

[24] K. E. Hallenius, P. Vas, and J. E. Brown, "The analysis of a saturated self excited asynchronous generator," *IEEE Transactions on Energy Conversion*, vol. 6, pp. 336–345, June 1991.

[25] T. F. Chan, "Steady state analysis of self-excited induction generators," *IEEE Transactions on Energy Conversion*, vol. 9, pp. 288–296, June 1994.

[26] T. F. Chan, "Analysis of a self-excited induction generator," *Electric Machines and Power Systems*, vol. 23, pp. 149–162, 1995.

[27] S. Rajakaruna and R. Bonert, "A technique for the steady state analysis of induction generator with variable speed," *IEEE Transactions on Energy Conversion*, vol. 8, pp. 757–761, Dec. 1993.

[28] S. P. Singh, B. Singh, and M. P. Jain, "Simplified approach for the analysis of self-excited induction generator," *J. Inst. Eng. (India) Electr. Eng.*, vol. 76, pp. 14–17, May 1995.

[29] T. F. Chan, "Analysis of self-excited induction generators using an iterative method," *IEEE Transactions on Energy Conversion.*, vol. 10, no. 3, pp. 502–507, Sep. 1995.

[30] D. K. Jain, A. P. Mittal, and B. Singh, "An efficient iterative technique for the analysis of self-excited induction generator," *J. Inst. Eng. (India) Electr. Eng.*, vol. 79, pp. 172–177, Feb. 1999.

[31] N. Ammasaigounden, M. Subbiah, and M. R. Krishnamurthy, "Wind-driven self- excited pole changing induction generators," *IEE Proceedings on Electric Power Applications*, vol. 133, no. 5, pp. 315–321, 1986.

[32] T. F. Chan, "Self-excited induction generators driven by regulated and unregulated turbines," *IEEE Transactions on Energy Conversion.*, vol. 11, no. 2, pp. 338–343, Jun. 1996.

[33] S. M. Alghuwainem, "Steady-state analysis of an isolated self-excited induction generator driven by regulated and unregulated turbine," *IEEE Transactions on Energy Conversion*, vol. 14, no. 3, pp. 718–723, Sep. 1999.

[34] S. M. Alghuwainem , "Steady state analysis of a self-excited induction generator self regulated by a shunt saturable reactor," *IEEE Transactions on Energy Conversion.*, 1997.

[35] S. M. Alghuwainem, "Steady-state analysis of a self-excited induction generator including transformer saturation," *IEEE Transactions on Energy Conversion.*, vol.14, pp. 667–672, Sept. 1999.

[36] K. S. Sandhu and S. K. Jain, "Operational aspects of self-excited induction generator using a novel model," *Electric Machines and Power Systems*, vol. 27, pp. 169–180, 1998.

[37] S. P. Singh, B. Singh, and M.P. Jain, "Performance characteristics and optimum utilization of a cage machine as capacitor excited induction generator," *IEEE Transactions on Energy Conversion.*, vol. 5, no. 4, pp. 679–685, Dec. 1990.

[38] L. Wang and C. H. Lee, "A novel analysis of the performance of an isolated self-excited induction generator," *IEEE Transactions on Energy Conversion.*, vol. 12, no. 2, pp. 109–115, Jun. 1997.

[39] B. Singh, L. Shridhar and C. S. Jha, "Improvements in the performance of self-excited induction generator through series compensation,"*IEE Proceeding on Generation, Transmission and Distribution*, vol. 146, no. 6, pp. 602–608, Nov. 1999.

[40] T. F. Chan and L. L. Loi, "Steady-state analysis and performance of a stand-alone three-phase induction generator with asymmetrically connected load impedances and excitation," *IEEE Transactions on Energy Conversion.*, vol. 16, pp. 327–333, Dec. 2001

[41] S. K. Kuo and L.Wang, "Analysis of isolated self-excited induction generator feeding a rectifier load," *IEE Proceeding on Generation, Transmission and Distribution*, vol. 149, no. 1, pp. 90–97, Jan. 2002.

[42] A. L. Alolah and M. A. Alkanthal, "Optimization based steady state analysis of three-phase self-excited induction generator," *IEEE Transactions on Energy Conversion.*, vol. 15, pp. 61–65, Mar. 2000.

[43] S. P. Singh, S. K. Jain and J.D. Sharma, "Voltage regulation optimization of compensated self excited induction generator with dynamic load," *IEEE Transactions on Energy Conversion.*, 2004, vol.19, no.4, pp.724-732.

[44] T. Ahmed and M. Nakaoka, "Static VAr compensator based terminal voltage control for standalone ac and dc outputted self excited induction generator," *IEE Proceeding on Power Electronics, Machines and Drives* ., vol. pp. 40-45. 2004,

[45] D. Joshi and K. S. Sandhu, "Performance analysis of three phase self excited induction generator using genetic algorithm," *Electric Power Components and Systems*, vol. 34, pp.461–470, 2006

[46] D. Joshi, K. S. Sandhu and M. Kumar Soni, "Constant voltage constant frequency operation for a self excited induction generator," *IEEE Transactions on Energy Conversion.*, vol. 21, no. 1, March 2006.

[47] N. Kumaresan, "Analysis and control of three-phase self-excited induction generators supplying single-phase AC and DC loads," *IEE Proceeding on Electric Power Application,* vol. 152, No. 3, May 2005

[48] A.-F. Attia, H. Soliman, M. Sabry, "Genetic algorithm based control system design of a self excited induction generator," *Acta Polytechnica*, vol. 46, no. 2, 2006.

[49] S. Velusami, and S. Singaravelu, "Steady state modelling and analysis of single-phase self excited induction generators," *Electric Power Components and Systems*, vol. 35, pp. 63–79, 2007

[50] G. K. Singh, A. S. Kumar and R. P. Saini, "Steady state modelling and analysis of six-phase self excited induction generator for renewable energy generation," *Electric Power Components and Systems*, vol. 38, pp. 137–151, 2010

[51] S Singaravelu and S Velusami, "Generalized steady state modelling and analysis of three phase self excited induction generators," *International Journal of Emerging Electric Power Systems*, vol. 3, Issue 2, Article 1080, 2005

[52] H. F. Soliman, A. A. Attia, S. M. Mokhymar and M. A. L. Badr, "Fuzzy algorithm for supervisory control of self excited induction generator," *JKAU: Engineering Science*, vol. 17, no. 2, pp. 19 – 40, 2006

[53] D. K. Palwalia and S. P. Singh, "Digital signal processor based fuzzy voltage and frequency regulator for self excited induction generator," *Electric Power Components and Systems*, vol.38, pp. 309–324, 2010

[54] Singh S.P and Jain M.P, "A new technique for the analysis of self excited induction generator, " *Electric Mach and Power Systems*, vol. 23, pp. 647- 656 1995.

[55] Chan T.F, "Performance analysis of a three-phase induction generator self excited with a single capacitance," *IEEE Transactions on energy conversions*, vol.14, no. 4, pp. 894-899, 1997.

[56] Chan T.F. and Lai L.L, "A novel single-phase self-regulated self-excited induction generator using a three-phase machine," *IEEE Transactions on energy conversions*, vol.16, no. 2, pp. 204-208, 2001.

[57] Chan T.F. and Lai L.L, "A novel excitation scheme for a standalone three phase induction generator supplying single phase loads," *IEEE Transactions on energy conversions*, 2004, vol.19, no. 1, pp. 136-142.

[58] Zadeh, L. "Fuzzy sets," *Information Control*,vol. 8, pp. 338-353, 1965.

[59] Vijayalakshmi. G.A., Rajsekaran. S, "Neural Networks, Fuzzy Logic, and Genetic Algorithms" synthesis and application.

[60] E. Cox, "The Fuzzy Systems Handbook", Morgan Kaufmann Publishers, 1998.

[61] George. J Klir/Boyuan, “Fuzzy Sets and Fuzzy Logic”, Prentice Hall of India Private Limited, New Delhi – 2000.

[62] T. J. Ross, “Fuzzy logic with engineering applications,”John wiley & Sons., India.

[63] Zadeh, L. (1976). ‘‘The concept of a linguistic variable and its application to approximate reasoning– Part 3,’’ *Information. Science.*, vol. 9, pp. 43–80, 1976.

[64] Zadeh, L. (1979). ‘‘A theory of approximate reasoning,’’ in J. Hayes, D. Michie, and L. Mikulich (eds.), *Machine Intelligence*, Halstead Press, New York, pp. 149–194.

[65] Hellendoorn, H. and Thomas, C. ‘‘Defuzzification in fuzzy controllers,’’ *Inteligent. Fuzzy Systems.*, vol. 1, pp. 109–123. 1993.

[61] Viachogiannis J.G, “Fuzzy logic applications in load flow studies,*” IEE proceedings*, 2001, vol. 148, no. 1, pp.34-40.

[62] Lo K.L., Lin Y.J and Siew W.H, “Fuzzy-logic method for adjustment of variable parameters in load-flow calculation,” *IEE Procedings*., vol. 146, no. 3, pp.276-281, 1999.

[63] Gupta P.V and Dhar P.C, Network analysis and synthesis, 1988, Dhanpat Rai & Sons, New Delhi, India.

[64] D.B. Watson, J . Arrillaga and T. Densem, "Controllable d.c. power supply for wind driven self-excited induction machines", *Proceedings of IEE*, vol. 126, no. 12, pp.1245-1248, 1979.

[65] R. Bonert and G. Hoops, "Standalone induction generator with terminal impedance controller and no turbine control", *IEEE Tranactions.* on *Energy Conversion*, vol. 5, pp.28-31, 1990.

[66] D.B. Watson and R.M. Watson, "Microprocessor control of a self-excited induction generator", *International Journal on Electrical Engineering Education*, vol. *22*, pp. 85-92, 1985.

[68] E. Profumo, B. Colombo and F. Mocci, "A frequency controller for induction generator in standby minihydro power plants", *4th International Conference on Electrical Machines and Drives*, vol. no. 310, pp.256-260, 1989.

[69] E. Bim, J. Szajner and Y. Burian, "Voltage compensation of an induction generator with long-shunt connection", *IEEE Transactions on Energy Conversion*, vol. 4, no. 3, pp.526-530, September 1989.

APPENDIX

Induction Machine 1 Data:

The following are the machine 1 parameters, the rating of the machine is 4-pole, 50Hz delta connected stator winding rated 230V, 12.5A and 5hp.

R_s = 0.0678 p.u,

R_r = 0.0769 p.u

X_{ls}=X_{lr}= 0.1204 p.u (at rated current)

V_{base}= rated phase voltage = 230 V

I_{base} = rated phase current = 7.217 A

Z_{base}= V_{base}/I_{base}=31.87 ohms

base power P_{base} = $V_{base} * I_{base}$ = 1.66 kW

base speed N_{base} = 1500 rpm

base frequency f_{base} =50 Hz

The variation of air-gap voltage (V_g) with magnetising reactance (X_m) is given as,

$V_g/F = 1.69 - 0.234X_m$

Induction Machine 2 Data:

Relevant experiments are carried out on a three-phase, 415 10% V, 10.1 A, 5.5 kW, 4-pole, delta connected, squirrel cage induction motor.

By the open circuit, short circuit, and synchronous speed test the calculated machine parameters are given as,

R_s = 0.0247 p.u.

R_r = 0.0633 p.u

X_{ls}=X_{lr}= 0.0633 p.u. (at rated current)

V_{base}= rated phase voltage = 415 V

I_{base} = rated phase current = 5.83 A

Z_{base}= V_{base}/I_{base} = 71.168 ohms

base power P_{base} = $V_{base} * I_{base}$ = 5.5 kW

base speed N_{base} = 1450 rpm

base frequency f_{base} =50 Hz

The variation of air-gap voltage (V_g) with magnetising reactance (X_m) is given as

$$V_g/_F = -0.0664{X_m}^2 + 0.4447{X_m}^2 - 1.1404X_m + 2.0272$$